Naunyn-Schmiedeberg's Arch Pharmacol (2006) 372: 413–431
DOI 10.1007/s00210-006-0043-8

REVIEW

J. Geyer · T. Wilke · E. Petzinger

The solute carrier family SLC10: more than a family of bile acid transporters regarding function and phylogenetic relationships

Received: 2 December 2005 / Accepted: 31 January 2006 / Published online: 16 March 2006

Abstract The solute carrier family 10 (SLC10) comprises two sodium-dependent bile acid transporters, i.e. the Na^+/taurocholate cotransporting polypeptide (NTCP; SLC10A1) and the apical sodium-dependent bile acid transporter (ASBT; SLC10A2). These carriers are essentially involved in the maintenance of the enterohepatic circulation of bile acids mediating the first step of active bile acid transport through the membrane barriers in the liver (NTCP) and intestine (ASBT). Recently, four new members of the SLC10 family were described and referred to as P3 (SLC10A3), P4 (SLC10A4), P5 (SLC10A5) and sodium-dependent organic anion transporter (SOAT; SLC10A6). Experimental data supporting carrier function of P3, P4, and P5 is currently not available. However, as demonstrated for SOAT, not all members of the SLC10 family are bile acid transporters. SOAT specifically transports steroid sulfates such as oestrone-3-sulfate and dehydroepiandrosterone sulfate in a sodium-dependent manner, and is considered to play an important role for the cellular delivery of these prohormones in testes, placenta, adrenal gland and probably other peripheral tissues. ASBT and SOAT are the most homologous members of the SLC10 family, with high sequence similarity (~70%) and almost identical gene structures. Phylogenetic analyses of the SLC10 family revealed that ASBT and SOAT genes emerged from a common ancestor gene. Structure–activity relationships of NTCP, ASBT and SOAT are discussed at the amino acid sequence level. Based on the high structural homology between ASBT and SOAT, pharmacological inhibitors of the ASBT, which are currently being tested in clinical trials for cholesterol-lowering therapy, should be evaluated for their cross-reactivity with SOAT.

Keywords Solute carrier family 10 · Na^+/taurocholate cotransporting polypeptide · Apical sodium-dependent bile acid transporter · Sodium-dependent organic anion transporter · Taurocholate · Oestrone-3-sulfate · Dehydroepiandrosterone sulfate · Phylogeny

J. Geyer (✉) · E. Petzinger
Institut für Pharmakologie und Toxikologie,
Justus-Liebig-Universität Gießen,
Frankfurter Strasse 107,
35392 Gießen, Germany
e-mail: Joachim.M.Geyer@vetmed.uni-giessen.de
Tel.: +49-641-9938404
Fax: +49-641-9938419

T. Wilke
Institut für Allgemeine und Spezielle Zoologie,
Justus-Liebig-Universität Gießen,
Heinrich-Buff-Ring 26–32,
35392 Gießen, Germany

Introduction

The HUGO Nomenclature Committee (HGNC) provides a list of so-called solute carrier (SLC) families comprising passive transporters, ion-coupled symporters, and antiporters in the plasma membrane and other cellular membrane compartments. A recent mini-review series of the SLC superfamily was published in 2004 in *Pflügers Archives European Journal of Physiology* (Vol. 447, No. 5) summarising physiological, pathophysiological, and pharmacological implications of each SLC family (Hediger et al. 2004). Currently, 43 SLC families are established in which a total of 319 human transporter genes and about the same number of rat and mouse transporter genes have been identified[1].

So far, solute carrier family 10 (SLC10) is termed the "sodium bile acid cotransporter family" and 2 years ago, this family comprised only two bile acid carriers, which belong to the group of sodium-coupled cotransporters in the plasma membrane. Both were cloned at the beginning of the 1990s and were termed Na^+/taurocholate cotransporting polypeptide (NTCP; SLC10A1) (Hagenbuch et al. 1990, 1991) and apical sodium-dependent bile acid transporter ASBT (SLC10A2), also called ileal Na^+/bile acid cotransporter (ISBT, IBAT) (Wong et al. 1994, 1995).

[1] For an actual list of SLC families see http://www.bioparadigms.org/slc.

Since 2004, four new members of the SLC10 family have been discovered and referred to as P3 (SLC10A3), P4 (SLC10A4), P5 (SLC10A5) and sodium-dependent organic anion transporter (SOAT; SLC10A6) (see Fig. 1 and Table 1) (Geyer et al. 2004; Hagenbuch and Dawson 2004). This article deals with sequence analyses, phylogenetic relationships and expression data of these new members. No experimental data supporting functional properties of P3, P4, and P5 are currently available. However, as demonstrated for SOAT, not all members of the SLC10 family are bile acid transporters (Geyer et al. 2004). Therefore, the grouping formerly called the "sodium bile acid cotransporter family" now has to be rearranged including the newly identified members.

With the identification of the ASBT-related SOAT and the NTCP-related P4 proteins, new perspectives arise for

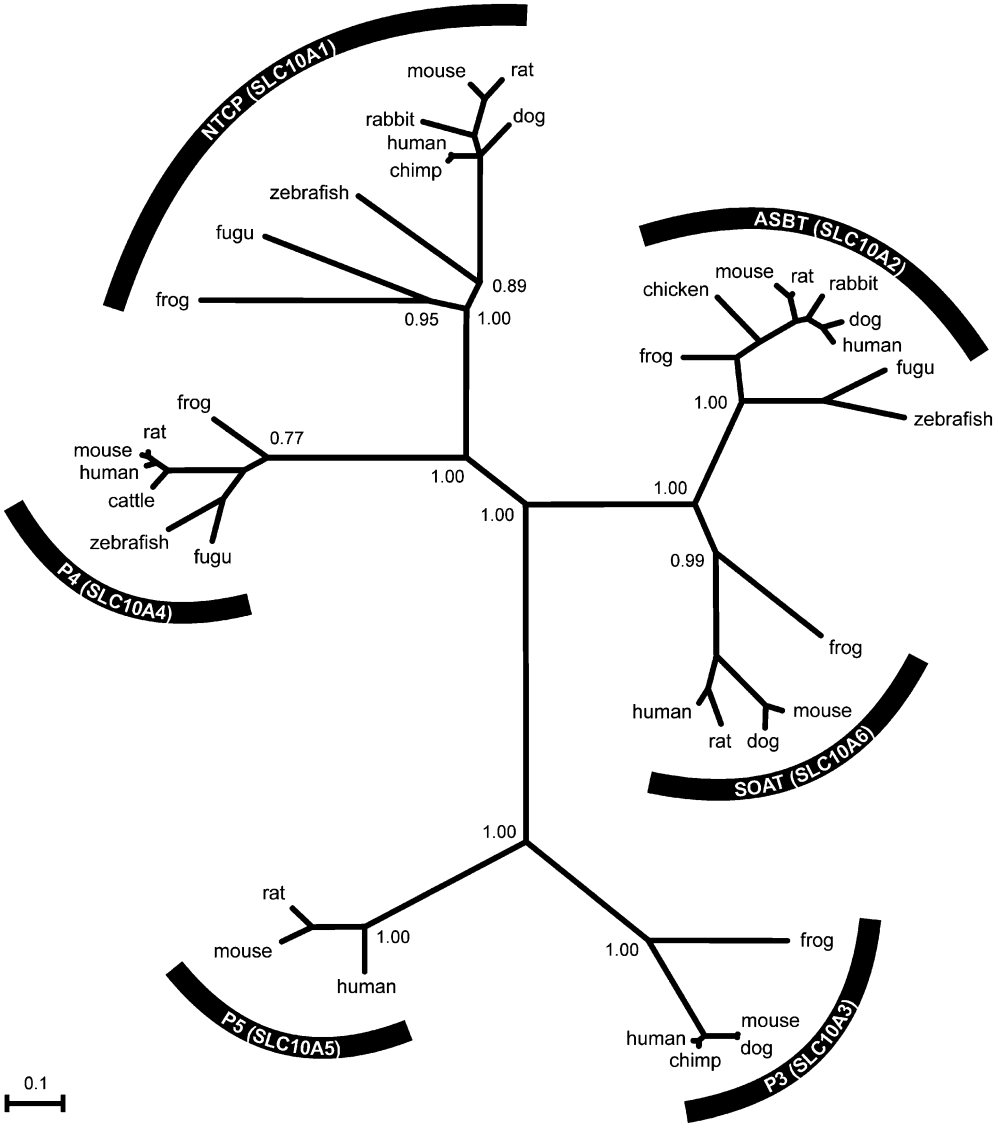

Fig. 1 Unrooted Bayesian protein tree of selected mammalian and non-mammalian members of the SLC10 transporter family (gene classifications for each subfamily are given in parentheses). Three of them (P3, P4 and P5) are still of unknown function. Multiple amino acid alignment of the indicated proteins was performed with the EBI *ClustalW* algorithm (http://www.ebi.ac.uk/clustalw/). The aligned set of sequences was truncated to the shortest sequence, resulting in 268 aligned amino acid positions. Phylogenetic reconstruction based on Bayesian inference was conducted using the software package MrBayes 3.1 (Ronquist and Huelsenbeck 2003). The best fixed-rate model of amino acid evolution was determined by model jumping among nine possible models. The model with the overall highest posterior probability was Cprev (Adachi et al. 2000). A total of 1,000,000 generations were sampled with the current tree saved at intervals of 10 generations. The 50% majority rule tree shown here was constructed from all sampled trees, with the first 2,500 trees (25,000 generations) ignored as burn-in. All major clades (i.e. protein subfamilies) are resolved with posterior probabilities greater than 0.95 (plotted at nodes). Posterior probabilities can be interpreted as the probability that the tree or clade is correct (Huelsenbeck and Rannala 2004). The *scale bar* represents the substitutions per site according to the model of amino acid evolution applied. Sequences from dog (*Canis familiaris*), frog (*Xenopus tropicalis*, *Xenopus laevis*), cattle (*Bos taurus*), chimp (*Pan troglodytes*), fugu (*Fugu rubripes*), zebrafish (*Danio rerio*) and chicken (*Gallus gallus*) were derived from Ensembl (http://www.ensembl.org) and HomoloGene (http://www.ncbi.nlm.nih.gov) orthologue predictions. Sequences from human, rat, mouse, and rabbit correspond to regular GenBank/EBI/DDBJ entries

Table 1 Amino acid sequence identities (*upper right*) and similarities (*lower left*) among the six human members of the SLC10 family. Values are percentages

	NTCP	P4	ASBT	SOAT	P3	P5	
NTCP		29.7	34.9	33.4	19.4	22.0	% identity
P4	53.5		29.1	28.7	23.0	21.7	
ASBT	62.8	54.4		41.8	18.8	22.0	
SOAT	62.6	51.5	69.7		21.1	20.1	
P3	39.2	44.9	38.8	36.8		33.9	
P5	44.6	48.7	43.4	41.3	60.9		
	% similarity						

Amino acid identity values were determined after pairwise optimal GLOBAL alignment with the BioEdit program version 7.0.5.2 (Hall 1999). For similarity calculations the DAYHOFF similarity matrix was used. Proteins were grouped according to their phylogenetic relationship (see below, "Phylogenetic relationships and evolutionary origin of the SLC10 family"). Amino acid sequences were taken from the following GenBank accession numbers: NTCP/NP_003040, P4/NP_689892, ASBT/NP_000443, SOAT/NP_932069, P3/NP_062822, and P5/NP_001010893

more detailed structure–activity analyses based on chimeric constructs and single amino acid replacements between these related proteins. This would be helpful to further localise the bile acid binding site in the ASBT, as this carrier is a clinically important drug target for cholesterol-lowering therapy.

Functional properties and expression patterns of the individual members of the SLC10 family

The bile acid transporters NTCP (SLC10A1) and ASBT (SLC10A2)

NTCP As the first member of the SLC10 family, the Na^+/taurocholate cotransporting polypeptide (Ntcp; Slc10a1) was isolated from rat liver mRNA by expression cloning using the *Xenopus laevis* oocytes expression system (Hagenbuch et al. 1990, 1991). Further orthologs were subsequently cloned from human (Hagenbuch and Meier 1994), mouse (Cattori et al. 1999) and rabbit (Kramer et al. 1999) livers. Human NTCP and rat/mouse Ntcps consist of 349 and 362 amino acids, respectively, and show an overall sequence identity of >73%. Additionally, mouse Ntcp gene encodes a second, less abundant splice variant with 317 amino acids and a shorter C-terminal end (Cattori et al. 1999). NTCP/Ntcps are exclusively expressed at the basolateral (sinusoidal) membrane of hepatocytes (Ananthanarayanan et al. 1994; Stieger et al. 1994; Kullak-Ublick et al. 1997). Here, they mediate sodium-coupled uptake of taurocholate and other bile acids with a Na^+:taurocholate stoichiometry of 2:1 (Hagenbuch and Meier 1996; Weinman 1997). Because more than 80% of the hepatic uptake of taurocholate appears in a sodium-dependent manner and Ntcp-specific antisense oligonucleotides blocked the Na^+-dependent taurocholate uptake in rat liver mRNA-injected *Xenopus laevis* oocytes by 95% (Hagenbuch et al. 1996), Ntcp represents the predominant taurocholate uptake system in hepatocytes (Trauner and Boyer 2003; Kullak-Ublick et al. 2004). More recently, expression of rat Ntcp was also detected in the luminal membrane of pancreatic acinar cells (Kim et al. 2002). Under normal physiological conditions, Ntcp may here be involved in the clearance of bile acids that leak to the terminal acini. However, bile acid uptake into pancreatic acinar cells is also associated with cell injury and pancreatic disorders (Kim et al. 2002). NTCP/Ntcp genes are located on chromosomes 14q24, 6q24 and 12 D1 in man, rat and mouse, respectively (Hagenbuch and Meier 1994; Cohn et al. 1995; Green et al. 1998). NTCP/Ntcp expression is regulated by a complex interplay of several ligand-activated receptors (retinoic acid receptor RARα, glucocorticoid receptor) and hepatic transcription factors (hepatocyte nuclear factors HNF1α, HNF4α, and HNF3β and small heterodimer partner SHP-1). This regulation is of particular interest under cholestatic conditions, where down-regulation of Ntcp contributes to the reduced hepatocellular accumulation of potentially toxic bile acids (for more detailed information see Meier and Stieger 2002, Trauner and Boyer 2003, Anwer 2004, Kullak-Ublick et al. 2004, Wagner and Trauner 2005).

ASBT The ileal counterpart to the hepatic NTCP is the apical sodium-dependent bile acid transporter (ASBT; SLC10A2). Asbt was originally cloned from a hamster intestinal cDNA library by expression cloning (Wong et al. 1994). Subsequently, human ASBT (Wong et al. 1995), rat Asbt (Shneider et al. 1995), rabbit Asbt (Kramer et al. 1999), and mouse Asbt (Saeki et al. 1999) were cloned from the ileum. The ASBT/Asbt proteins of all mentioned species consist of 348 amino acids and show an overall amino acid identity of >80%. However, sequence identity to the NTCP is relatively low, at 35% (see Table 1). Similar to NTCP/Ntcp, ASBT/Asbt transports conjugated bile acids with high affinity in a sodium-dependent manner (Wong et al. 1994, 1995; Craddock et al. 1998). This transport is electrogenic and shows a 2:1 Na^+/bile acid coupling stoichiometry (Weinman et al. 1998). In contrast to the basolateral localisation of Ntcp, Asbt is highly expressed in the apical brush border membrane of enterocytes of the terminal ileum (Shneider et al. 1995). Here, Asbt is associated with the 14 kilodalton cytoplasmic ileal lipid-binding protein ILBP, which is the

predominant bile acid binder in the cytosol of ileal enterocytes (Stengelin et al. 1996; Kramer et al. 1997, 2001a,b). In the intestine ASBT is thought to be the major route for active bile acid uptake as emphasised by loss-of-function mutations in the human ASBT gene that cause primary bile acid malabsorption, an interruption of the enterohepatic circulation of bile acids, and reduced plasma LDL cholesterol levels (Wong et al. 1995; Oelkers et al. 1997). Similarly, genetically engineered knockout mice with a targeted deletion of the Asbt gene ($Slc10a2^{-/-}$) showed profound intestinal bile acid malabsorption and an increase in faecal bile acid excretion (Dawson et al. 2003). Further analyses of mRNA and protein expression revealed that Asbt is also expressed in the apical membrane of the renal proximal convoluted tubule, where it might be important for tubular reabsorption of bile acids that are filtrated by the glomeruli (Christie et al. 1996). Asbt expression was also detected in the apical membrane of cholangiocytes in the liver bile duct epithelium (Alpini et al. 1997; Lazaridis et al. 1997). Here, an additional truncated form of Asbt (so-called t-Asbt) is expressed, which contains 154 instead of 348 amino acids and has a molecular weight of 19 kDa. t-Asbt was localised to the basolateral plasma membrane of cholangiocytes and was shown to mediate bile acid efflux (Lazaridis et al. 2000). The physiological role of Asbt expression in cholangiocytes is not clear. Probably, apical Asbt and basolateral t-Asbt expressions permit a cholehepatic shunt for bile acids by transporting them across the bile duct epithelium. ASBT/Asbt genes are on chromosomes 13q33, 16q12, and 8 A1 in man, rat and mouse, respectively (Wong et al. 1996). Expression of the Asbt gene is under control of hepatocyte nuclear factor HNF1α. Hence, in the HNF1α knockout mouse Asbt expression was undetectable in the ileum at RNA and protein levels (Shih et al. 2001). Furthermore, Asbt expression is regulated by bile acids through an activation of the nuclear farnesoid X receptor FXR. However, whereas in rabbits, mice and humans Asbt expression is under negative-feedback control by bile acids (Chen et al. 2003; Neimark et al. 2004; Li et al. 2005), in rats Asbt expression was not regulated by alterations of ileal bile acid concentration (Arrese et al. 1998). This could be explained by the absence of the liver receptor homologue-1 (LRH-1) transcription binding site in the rat Asbt promoter, by which FXR regulates Asbt expression in rabbits and mice (Chen et al. 2003; Li et al. 2004).

Membrane insertion and sorting of NTCP and ASBT

Based on bioinformatic predictions and experimental data, it has been shown that NTCP and ASBT have an extracellular N-terminus, an odd number of transmembrane helices (seven or nine) and a cytoplasmic C-terminus (Hagenbuch et al. 1991; Hagenbuch and Meier 1994; Stieger et al. 1994; Dawson and Oelkers 1995; Hallén et al. 1999; Hallén et al. 2002b; Zhang et al. 2004). Several potential N-glycosylation sites are present in NTCP, ASBT and SOAT proteins, and site-directed mutagenesis has revealed that only N^{5} and N^{11} in rat Ntcp (Hagenbuch 1997), and N^{10} in human ASBT (Zhang et al. 2004) are glycosylated. These findings clearly placed the N-terminus of these proteins to the extracellular surface of the plasma membrane. Furthermore, antibodies that were raised against the C-terminal part of Ntcp were only reactive in detergent-permeabilised cells, indicating that the C-terminal part of Ntcp has to be located intracellularly (Ananthanarayanan et al. 1994; Stieger et al. 1994). However, there is still controversy about the exact number of transmembrane helices. Using N-glycosylation-scanning mutagenesis, Zhang and coworkers strongly suggested a model with seven transmembrane domains for human ASBT (Zhang et al. 2004). In contrast, a nine-transmembrane domain arrangement was found by Hallén and coworkers for human ASBT and NTCP (Hallén et al. 1999, 2000, 2002b). However, it remains unclear whether all of these nine transmembrane segments cross the membrane or whether two of them fold as lipid-buried re-entrance loops in the plasma membrane (Hallén et al. 2002b; Zahner et al. 2003).

Several experimental studies were performed to clarify the molecular basis for the opposite sorting directions of ASBT and NTCP in the apical and basolateral membrane domain, respectively. For rat Asbt, it has been established that the signal for the apical sorting is located in the cytoplasmic C-tail. Truncation of Asbt by the 40 carboxyterminal amino acid residues nearly abolished sorting to the apical plasma membrane (Sun et al. 1998). More detailed analyses identified the potential phosphorylation residues S^{335} and T^{339} as the main determinants for the apical direction of membrane expression in Asbt (Sun et al. 2003). In contrast, removal of the carboxyterminal 56 amino acids of rat Ntcp did not completely block basolateral sorting in polarised MDCK cells and did not affect bile acid transport function of Ntcp (Sun et al. 1998, 2001). Finally, Y^{307} and Y^{321} were identified in the C-tail of rat Ntcp to be critical amino acid residues for its basolateral expression. Site-directed mutagenesis of these tyrosines to alanines redirected these mutant transporters mainly toward the apical domain of transfected MDCK cells (Sun et al. 2001).

Furthermore, cAMP-induced dephosphorylation of Ntcp was shown to stimulate transport function by increasing Ntcp translocation to the plasma membrane (Mukhopadhayay et al. 1997; Dranoff et al. 1999). Protein phosphatase 2B, a calcium/calmodulin-dependent serine and threonine protein phosphatase, was identified to be involved in this process (Webster et al. 2002). Using a series of threonine-to-alanine and serine-to-alanine mutants of rat Ntcp, Anwer and coworkers recently identified the site of phosphorylation of this carrier. In these experiments, only the S226A mutant significantly reduced Ntcp phosphorylation and increased Ntcp membrane retention, indicating that S^{226} in the third intracellular loop of the protein is the main site of Ntcp phosphorylation. Accordingly, cAMP may increase Ntcp translocation to the plasma membrane mainly by S^{226} dephosphorylation (Anwer et al. 2005).

Substrate specificities of NTCP and ASBT

The transport functions of NTCP/Ntcps and ASBT/Asbts were extensively studied in several cell systems. In general, both carriers transport all physiological dihydroxy and trihydroxy bile acids, with a preference for the taurine and glycine conjugates above the unconjugated forms. Furthermore, affinities and uptake rates for the dihydroxy bile acids (e.g. taurochenodeoxycholate, taurodeoxycholate) were normally higher than for the trihydroxy bile acids (i.e. cholate, taurocholate and glycocholate) (Craddock et al. 1998; Schroeder et al. 1998; Kramer et al. 1999; Kullak-Ublick et al. 2000a; Hata et al. 2003). Exceptionally, ASBT has a lower affinity for the dihydroxy bile acid tauroursodeoxycholate than for taurocholate (Craddock et al. 1998). Due to their transport characteristics and expression pattern, NTCP and ASBT are essentially involved in the maintenance of the enterohepatic circulation of bile acids mediating the first step in the cellular uptake of bile acids through the membrane barriers in the liver (NTCP) and intestine (ASBT). Several reviews deal with this topic and are recommended for further information (Shneider 2001; Meier and Stieger 2002; Trauner and Boyer 2003; Kullak-Ublick et al. 2004; Marin et al. 2005).

In contrast to ASBT, substrate specificity of NTCP is not limited strictly to bile aids. NTCP/Ntcp also transports steroid sulfates such as oestrone-3-sulfate and DHEAS, bromosulfophthalein and the drug-conjugate chlorambucil-taurocholate (Kullak-Ublick et al. 1997; Craddock et al. 1998; Schroeder et al. 1998; Kullak-Ublick et al. 2000b; Hata et al. 2003) (see Table 2). However, in comparison with the transport of bile acids, Ntcp-mediated uptake of steroid sulfates is relatively low (Meier et al. 1997; Schroeder et al. 1998; Kullak-Ublick et al. 2000b). Further differences between the substrate specificities of NTCP and ASBT exist for sulfated bile acids, which are structurally very similar to the sulfated sex steroids. Chenodeoxycholate-3-sulfate is not transported by ASBT, but is a substrate of NTCP (Craddock et al. 1998). Similarly, taurolithocholate-3-sulfate had a much higher inhibitory potency to rabbit Ntcp (IC_{50}=0.8 μM) than to rabbit Asbt (IC_{50}=9.1 μM) (Kramer et al. 1999).

A better understanding of substrate recognition and binding on rabbit Ntcp and Asbt was obtained by intensive inhibitory screening analyses with a series of 23 bile acid analogues in rabbit ileal brush border membrane vesicles and stably transfected CHO cells (Kramer et al. 1999). Generally, most tested bile acids had a higher affinity to Ntcp than to Asbt. This finding was most striking for the bile acids carrying a hydroxy group at position 6 (dehydrotaurocholate and ω-muritaurocholate). However, comparable affinities to both transporters were found for

Table 2 Substrate specificities of NTCP, ASBT, and SOAT

Carrier	Substrates / inhibitors	Reference
NTCP/Ntcp	*Bile acids*: Cholate, taurocholate (6–34 μM), glycocholate (27 μM), NBD-taurocholate, taurochenodeoxycholate (5 μM), taurodeoxycholate (7.4 μM), tauroursodeoxycholate (14 μM), taurohyodeoxycholate (6.8 μM), tauromurocholate *Bile acid sulfate*: Chenodeoxycholate-3-sulfate *Steroid sulfates*: Oestrone-3-sulfate (27–60 μM), DHEAS *Others*: BSP (3.7 μM), chlorambucil-taurocholate (11 μM) *Inhibitors*: Cyclosporin {1 μM}[a], (R)-propranolol {5.5 μM}[a], (S)-propranolol {6.1 μM}[a], BSP {7.3 μM}[a], furosemide {15 μM}[a], DIDS {3.1 μM}[b], 17β-oestradiol-3-sulfate, taurolithocholate-3-sulfate {0.8 μM}[b]	Boyer et al. 1994, Hagenbuch and Meier 1994, Platte et al. 1996, Kullak-Ublick et al. 1997, Craddock et al. 1998, Schroeder et al. 1998, Kim et al. 1999, Kramer et al. 1999, Kullak-Ublick et al. 2000b, Hata et al. 2003
ASBT/Asbt	*Bile acids*: Cholate (33–37 μM), taurocholate (12–18 μM), chenodeoxycholate [3.3 μM], taurochenodeoxycholate [6.1 μM], glycochenodeoxycholate (5.7 μM), deoxycholate [6.3 μM], taurodeoxycholate [17.2 μM], glycodeoxycholate (2 μM), ursodeoxycholate [75 μM], tauroursodeoxycholate [28 μM], glycoursodeoxycholate (4.1 μM) *Bile acid sulfate*: Chenodeoxycholate-3-sulfate (n.t.) *Inhibitors*: BSP [144 μM][c], cyclosporin A [25 μM][c] *Specific inhibitors*: Dimeric bile acid analogues (e.g. PB3, S 0960), benzothiazepine derivatives (e.g. 2164U90, 264W94), benzothiepine derivatives (e.g. SC-435), naphthol derivatives (e.g. S 8921), 4-oxo-1-phenyl-1,4,-dihydroquinoline derivatives	Lewis et al. 1995, Root et al. 1995, Oelkers et al. 1997, Craddock et al. 1998, Weinman et al. 1998, Baringhaus et al. 1999, Kramer et al. 1999, Tollefson et al. 2000, Root et al. 2002, West et al. 2002, Kurata et al. 2004, Huang et al. 2005
SOAT/Soat	*Bile acids*: Taurocholate (n.t.), cholate (n.t.)*, chenodeoxycholate (n.t.)* *Steroid sulfates*: Oestrone-3-sulfate (31 μM), DHEAS (30 μM), pregnenolone sulfate *	Geyer et al. 2004, *Geyer et al., unpublished data

K_m values are given in parentheses; K_i values are shown in squared brackets; n.t., not transported
[a]IC_{50} values for NTCP-mediated taurocholate uptake (Kim et al. 1999)
[b]IC_{50} values for NTCP-mediated taurocholate uptake (Kramer et al. 1999)
[c]Noncompetitive inhibitors

the most abundant physiological bile acids taurocholate, taurodeoxycholate, taurochenodeoxycholate and glycocholate (Kramer et al. 1999). Using an additional set of 17 chemically diverse inhibitors of Asbt (containing no bile acid monomers), a three-dimensional QSAR pharmacophore model was developed for Asbt. According to this model, the five-membered D-ring of the steroid nucleus, the 21-methyl group of the bile acid side chain, the hydroxy group in position 12α or 7α, and the negative charge of the side chain, are essential for bile acid recognition and binding by Asbt. However, neither the 3α-hydroxy group of the steroid nucleus nor the cis-oriented A-ring is important for substrate recognition by Asbt (Baringhaus et al. 1999). This pharmacophore model is in good agreement with another QSAR model for Asbt that was previously developed by Swaan and coworkers using a series of 30 bile acid derivatives in the inhibition studies (Swaan et al. 1997).

Pharmacological inhibition of the ASBT

Bile acid synthesis in the liver is under inhibitory feedback regulation of bile acids, which mostly derive from the enterohepatic re-circulation. However, reduced bile acid reflux from the intestine is able to increase the expression of the hepatic cholesterol 7α-hydroxylase (CYP7A1), a member of the superfamily of cytochrome P450 enzymes, which is the rate-limiting enzyme in the classical bile acid synthetic pathway (Dietschy et al. 1993; Bjorkhem et al. 1997; Vlahcevic et al. 1999; Chiang et al. 2000). Accordingly, impairment of the ileal bile acid carrier ASBT by mutations or specific inhibitors will increase bile acid synthesis in the liver and thereby lowering plasma cholesterol levels. This phenomenon was documented in patients with loss-of-function mutations in ASBT (i.e. L243P, T262M, and P290S). In these patients, primary bile acid malabsorption is clinically concomitant with diarrhoea and steatorrhoea (Oelkers et al. 1997).

Similarly, several specific ASBT inhibitors were able to significantly lower plasma cholesterol levels and/or prevent atherosclerosis in animal studies, supporting the feasibility of a cholesterol-lowering therapy by blocking the ASBT transport function (Root et al. 1995; Higaki et al. 1998; Ichihashi et al. 1998; West et al. 2002; Li et al. 2004; Tremont et al. 2005). Several classes of ASBT inhibitors were developed (see Fig. 2). The first class of compounds comprised dimeric bile acid analogues where two bile acid molecules were coupled via spacer. These compounds were able to block simultaneously ligand binding sites of two ASBT molecules from the cell surface without being translocated (Wess et al. 1994; Kramer and Wess 1996; Baringhaus et al. 1999). A second class of ASBT inhibitors contains several benzothiazepine derivatives. 2164U90[2], for example, is a competitive inhibitor of murine Asbt (Root et al. 1995). In rats and mice, oral administration of 1–25 mg/kg b.w. 2164U90 significantly lowered plasma LDL and VLDL cholesterol in diet-induced hypercholesterolaemic animals (Lewis et al. 1995). However, 2164U90 was shown to have species-specific selectivity as K_i value was 0.068 μM for mouse Asbt, but 10 μM for the human protein. At the molecular level, two single amino acid residues were identified in human ASBT to be responsible for this shift in affinity. Replacement of S294 and I295 by the corresponding amino acid residues of mouse Asbt (T294 and V295) highly enhanced the affinity of 2164U90 towards ASBT (Hallén et al. 2002a). Further development for clinical usage was 264W94[3], synthesised by adding two additional methoxy groups. This compound competitively inhibited ASBT with K_i of 0.2 μM and was a ~500-fold more potent inhibitor than 2164U90 of the ileal bile acid absorption in rats in vivo (Root et al. 2002). More recently, large series of benzothiepine derivatives[4] were synthesised and several compounds of this group potently inhibit Asbt with IC_{50} values in the low nanomolar range (Huang et al. 2005; Tremont et al. 2005). One reagent of this group, SC-435[5], was identified as a potent and nonabsorbed inhibitor of ASBT (IC_{50}=1.5 nM). Several in vivo studies were performed with SC-435 treatment in Hartley guinea pigs, miniature pigs, New Zealand White rabbits and dogs. Concordantly, these studies found an increase of faecal bile acid excretion, decreased total and LDL-cholesterol plasma levels, and enhanced expression of the hepatic LDL receptor, secondary to the upregulation of hepatic cholesterol 7α-hydroxylase (CYP7A1) expression (Huff et al. 2002; West et al. 2002, 2003; Bhat et al. 2003; Telford et al. 2003; Li et al. 2004).

Besides benzothiazepine and benzothiepine derivatives, several naphthol derivatives potently inhibit Asbt as well. The strongest compound in this group is S 8921[6], which is a mixed competitive and non-competitive ASBT inhibitor with an IC_{50} value of 2.5 μM (Hara et al. 1997; Tollefson et al. 2000). In vivo studies with S 8921 were performed in hamsters, rats and rabbits and revealed an upregulation of the cholesterol 7α-hydroxylase and HMG-CoA reductase activities, an increase in the hepatic LDL-receptor expression concomitant with reduced plasma cholesterol levels (Higaki et al. 1998; Ichihashi et al. 1998). Furthermore, in cholesterol-fed New Zealand White rabbits, S 8921 treatment efficiently suppressed the development of hypercholesterolaemia and reduced the severity of coronary atherosclerosis (Higaki et al. 1998). Finally, a fourth class of 4-oxo-1-phenyl-1,4-dihydroquinoline-based ASBT in-

[2] (-)-(3R,5R)-*trans*-3-butyl-3-ethyl-2,3,4,5-tetrahydro-5-phenyl-1,4-benzothiazepine 1,1-dioxide

[3] (-)-(3R,5R)-*trans*-3-butyl-3-ethyl-2,3,4,5-tetrahydro-7,8-dimethoxy-5-phenyl-1,4-benzothiazepine 1,1-dioxide

[4] 3R,3R′-2,3,4,5-tetrahydro-5-aryl-1-benzothiepin-4-ol 1,1-dioxides

[5] 1-[4-[4[(4*R*,5*R*)-3,3-dibutyl-7-(dimethylamino)-2,3,4,5-tetrahydro-4-hydroxy-1,1-dioxido-1-benzothiepin-5-yl]phenoxy]butyl]-4-aza-1-azoniabicyclo[2.2.2]octane methanesulfonate

[6] Methyl-1-(3,4-dimethoxyphenyl)-3-(3-ethylvaleryl)-4-hydroxy-6,7,8-trimethoxy-2-naphthoate

hibitors was developed. Compounds of this group showed inhibitory potency with IC_{50} values of about 1 μM and were able to reduce non-HDL-cholesterol levels in chow-fed Syrian golden hamsters (Kurata et al. 2004).

In conclusion, several chemically divergent molecules are potent inhibitors of ASBT and several reagents of this group are promising candidates for the treatment of hypercholesterolaemia. Based on the high structural homology between ASBT and SOAT, these ASBT inhibitors need to be evaluated for their inhibition potency on SOAT.

The sodium-dependent organic anion transporter SOAT (SLC10A6)

Two years ago, we reported cloning of a new functional member of the SLC10 family and called it SOAT (sodium-dependent organic anion transporter) (Geyer et al. 2004). SOAT/Soat of man, rat and mouse consist of 370–377 amino acids, which is very similar to the sequence size of NTCP/Ntcp (349–362) and ASBT/Asbt (348 amino acids). Sequence identity and similarity of human SOAT are highest to human ASBT, at 41.8% and 69.7%, respectively (Table 1). These are the highest homology values between any two members of this transporter family, indicating that SOAT and ASBT are so far the most homologous proteins of the SLC10 family at the sequence level. However, in contrast to NTCP and ASBT, SOAT is not a bile acid transporter. Instead, it specifically transports steroidsulfates such as oestrone-3-sulfate and DHEAS (Geyer et al. 2004). This transport is highly sodium-dependent, suggesting a symport transport mechanism of the substrate with Na^+, as has been established for NTCP and ASBT. According to the membrane topology of NTCP and ASBT, SOAT structure was predicted with seven or nine transmembrane domains.

Whereas the physiological function of NTCP and ASBT is well understood, this is not clear for SOAT. The SOAT substrate oestrone-3-sulfate serves as a non-active form of oestrogens in the circulation and can be metabolised after cellular uptake to active oestrogens such as oestrone, oestradiol, and oestriol (Platia et al. 1984; Howarth et al. 2002). Another SOAT substrate, DHEAS, is synthesised and secreted by the adrenal cortex and can be reversibly hydrolysed to the corresponding free steroid DHEA. DHEAS serves as the principal conjugated pro-hormone for the biosynthesis of oestrogenic and androgenic steroids in peripheral tissues (Baulieu 1996; Labrie et al. 1998). Plasma concentrations of DHEAS are in the range of 2–10 μM in young adults (Baulieu 1996), which is near the K_m for in vitro DHEAS transport by Soat (K_m=30 μM). Against this background, SOAT could have an important physiological function for the delivery of oestrone-3-sulfate and DHEAS into hormone-dependent tissues, such as testis, placenta, and adrenal gland (Geyer et al. 2004). To prove this concept further characterisation of SOAT expression and function is mandatory.

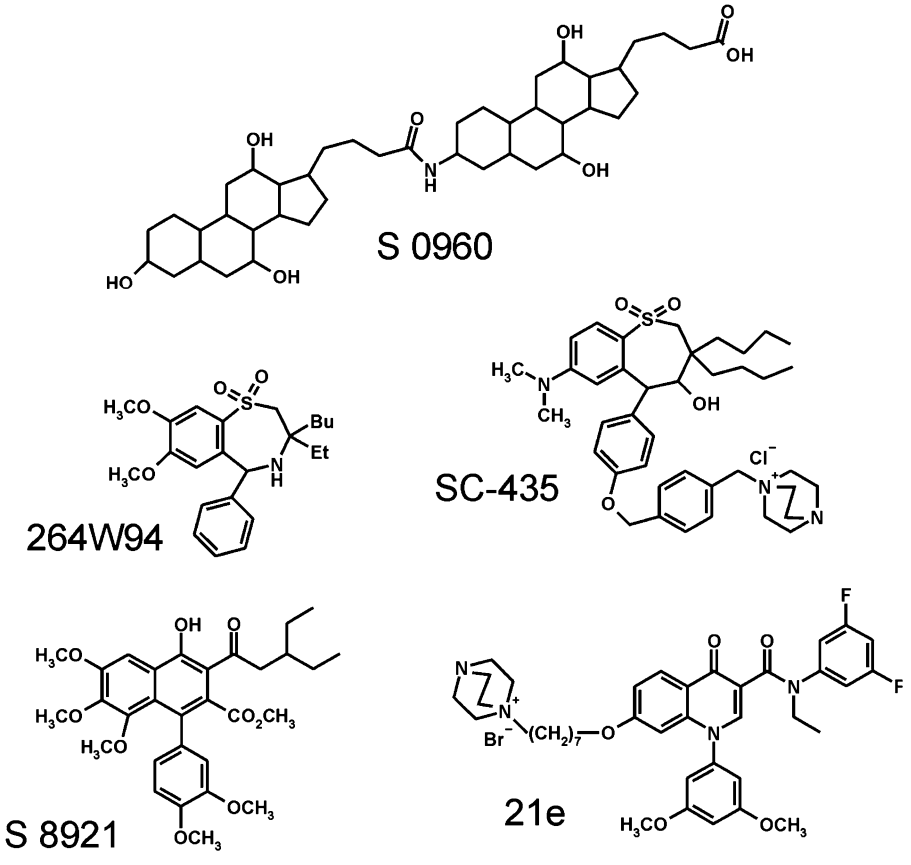

Fig. 2 Different chemical classes of inhibitors of the ABST: dimeric bile acid analogues (e.g. S 0960), benzothiazepine derivatives (e.g. 264W94), bezothiepine derivatives (e.g. SC-435), naphthol derivatives (e.g. S 8921), and 4-oxo-1-phenyl-1,4,-dihydroquinoline derivatives (e.g. compound 21e)

Orphan members of the SLC10 family: P3 (SLC10A3), P4 (SLC10A4) and P5 (SLC10A5)

Besides NTCP, ASBT and SOAT, recently three orphan transporters have been mentioned that also belong to the SLC10 transporter family, i.e. P3, P4 and P5 (Hagenbuch and Dawson 2004). However, up to now there are no experimental data indicating that they have any function as solute carriers.

The P3 gene was identified in 1988, before NTCP and ASBT were cloned. It is located 40 kb downstream from the human G6PD gene (glucose-6-phosphate dehydrogenase) and has a CpG island in its promoter region (Alcalay and Toniolo 1988). CpG islands are typically associated with housekeeping genes or genes with tissue-specific expression (Gardiner-Garden and Frommer 1987). The P3 cDNA was cloned from placenta and teratocarcinoma cDNA libraries. Further P3 expression was detected in human fibroblasts, HeLa cells, human T-lymphocytes, Ca-Ma (human mammary carcinoma cells), PA-1 (human neuroblastoma cells), COS-1 cells and JEG (human choriocarcinoma cells) (Alcalay and Toniolo 1988). The P3 gene is divided into two exons of 350 bp and 1806 bp. The latter contains the full open reading frame of 1430 bp coding for the P3 protein of 477 amino acids. By Southern blot analysis with a P3 cDNA probe, P3-related sequences were also detected in the genomes of several animal species (monkey, mouse, rat, cattle, horse, chicken, frog, *D. melanogaster*) and yeast

Table 3 Human and rodent members of the SLC10 transporter family

Gene name	Protein name	Species	Tissue distribution	Gene locus	GenBank Accession
SLC10A1	NTCP	*H. sapiens*	Liver (basolateral membrane)[a] and pancreas (tubuli)	14q24	NM_003049
		R. norvegicus		6q24	NM_017047
		M. musculus		12 D1	NM_011387
SLC10A2	ASBT	*H. sapiens*	Ileum (apical membrane)[a], kidney (proximal tubulues)[a] and cholangiocytes (apical membrane)[a]	13q33	NM_000452
		R. norvegicus		16q12	NM_017222
		M. musculus		8 A1	NM_011388
SLC10A3	P3	*H. sapiens*	Human fibroblasts, human T-lymphocytes, HeLa, Ca-Ma, PA-1, COS-1, and JEG cells[a] Placenta, small intestine, pancreas, cervix, kidney, uterus, and others[b] Placenta, teratocarcinoma, brain neuroblastoma[c]	Xq28	NM_019848
		R. norvegicus [d]	Heart, ovary, pituitary gland[b] Ovary[c]	Xq37	NM_001024368
		M. musculus	Pineal gland, ear, female genital tract, mammary gland, thymus, kidney, and others[b] Mammary tumour, thymus[c]	X A7	NM_145406
SLC10A4	P4	*H. sapiens*	Brain, eye, soft tissue[b] Brain neuroblastoma[c]	4p12	NM_152679
		R. norvegicus	Adrenal gland[c]	14p11	NM_001008555
		M. musculus [d]	Vascular system, ganglia, stomach, diencephalon, cortex, brain stem, and others[b] Eyeball, sympathetic ganglion[c]	5 C3	NM_173403
SLC10A5	P5	*H. sapiens*	Brain, liver[c]	8q21	NM_001010893
		R. norvegicus	Brain, eye[b] Small intestine[c]	2q23	NM_001025280
		M. musculus	Liver, kidney, pancreas, thymus[b] Kidney, liver[c]	3 A1	NM_001010834
SLC10A6	SOAT	*H. sapiens*	Adrenal gland[c]	4q21	NM_197965
		R. norvegicus	Brain, heart, kidney, lung, skeletal muscle, spleen, testis, adrenal gland, small intestine[a]	14p22	NM_198049
		M. musculus	Vascular system, respiratory tract, female genital tract, bladder, heart, mammary gland, spleen[b] Uterus, liver, lung[c]	5 E5	NM_029415

[a]Experimental evidence; [b]based on EST sequence data, [c]full-length cDNA cloning, [d]unclassified gene

SLC10 gene classification as shown in this table is implemented for all human genes by the HUGO Gene Nomenclature Committee HGNC (http://www.gene.ucl.ac.uk/nomenclature/), for the mouse genes by the Mouse Genome Informatics Database MGI (http://www.informatics.jax.org/) and for the rat genes by the Rat Genome Database RGD (http://www.rgd.mcw.edu/). Currently, only mouse P4 and rat P3 genes are not yet classified

(*S. cerevisiae, H. capsulatum*). Therefore, it was concluded that the P3 gene has been considerably conserved during evolution and codes for a protein that probably has a housekeeping function (Alcalay and Toniolo 1988). However, still no specific function of the P3 gene is known. This gene was retrospectively included into the SLC10 family (SLC10A3) because of a certain sequence homology to NTCP and ASBT (Hagenbuch and Dawson 2004).

The second orphan transporter is called P4 (SLC10A4). Its sequence length is much greater than those of NTCP, ASBT and SOAT, and amino acid identities (29–30%) and similarities (52–54%) are almost identical to NTCP, ASBT and SOAT (Table 1). P4 expression seems to be dominant in nervous tissue. Full-length cDNA sequences for P4 were cloned from a neuroblastoma-derived cDNA library in man, from sympathetic ganglion in mouse and from adrenal gland in rat (Table 3). Even human- and mouse-derived EST data supports this expression characteristics. Currently it remains unclear whether P4 is a physiologically relevant solute carrier for the transport of neurosteroids or other neuroactive molecules, but interestingly, P4 does not transport bile acids (Geyer et al., unpublished data).

Finally, the 434–438 amino acid P5 protein was cloned from man, rat and mouse having high sequence identity (34%) and similarity (61%) to P3 (Table 1). Expression data of P5 (derived from full-length cDNA cloning and EST analyses) indicates that P5 is expressed most highly in the liver, kidney and intestine, which is very similar to the expression pattern of ASBT (Table 3). However, P5 has not been subjected to intensive experimental expression analysis and transport function of P5 has still to be proven.

Because of the high sequence similarities of P3, P4 and P5 to NTCP, ASBT and SOAT (>37%), these three orphan transporters were predicted to have also Na^+-dependent transport function (see GenBank commentaries). However, they show clear differences from NTCP, ASBT and SOAT in terms of protein lengths and genomic organisation (see Figs. 3 and 7). No published experimental data indicate that they function as solute carriers, and hence no transportates are known.

Structure-activity relationships of the SLC10 members

Currently, there is only limited information about the structure-based transport relationships of the SLC10 family members. The ligand-binding sites of NTCP, ASBT and SOAT have not been definitely localised and the exact transport mechanism remains unknown. However, much detailed information can be obtained from a direct sequence comparison concerning differences or similarities in transport function. Most noticeably, C- and N-terminal domains of the six SLC10 members NTCP, ASBT, SOAT, P3, P4 and P5 have completely different amino acid sequences. In contrast, a highly homologous core region exists representing the transmembrane part of the proteins (see Fig. 3). Lengths of the C-termini, which are localised intracellularly, are relatively similar to each other, but all six members differ markedly in the lengths of their N-terminal domains, which are at the cell surface. More precisely, P3, P4 and P5 contain N-termini of 100–180 amino acids, whereas those in NTCP, ASBT and SOAT are only 20–30 amino acids long. Considering only NTCP, ASBT and SOAT sequences, identity alignment score is best at a highly conserved sequence domain that starts at amino acid position 114 for NTCP/Ntcp and at position 121 for ASBT/Asbt and SOAT/Soat (Fig. 4). The consensus sequence of this domain establishes the NTCP/ASBT/SOAT signature motif (Geyer et al. 2004). This motif is located in transmembrane domain III of NTCP, ASBT, and SOAT.

Concerning sequence (dis)similarities among NTCP, ASBT and SOAT, the question arises of which structural requirements are necessary for these proteins to serve as bile acid and/or steroidsulfate carriers. In the early 1990s, we showed that organic SH-group reagents inactivated Na^+-dependent and Na^+-independent bile acid uptake into isolated rat hepatocytes. This transport blockade was reversed by several mercapto-compounds (e.g. DTT) that are able to reduce S-S bridges (Blumrich and Petzinger 1990, 1993). Similar results were obtained by Kramer and coworkers for the Na^+-dependent bile acid uptake in the ileum from rabbit small intestine (Kramer et al. 1992). From these studies, it was suggested that cysteine residues in the hitherto unidentified bile acid carrier proteins are important for substrate binding and translocation. With the molecular identification of NTCP and ASBT, these findings were re-evaluated with an almost complete series of cysteine to alanine mutations in human ASBT (Banerjee et al. 2005), human NTCP (Hallén et al. 2000), mouse Asbt and Ntcp (Saeki et al. 2002) and rat Ntcp (Zahner et al. 2003). Concordantly, these studies identified the conserved cysteine residue C^{266} in NTCP/Ntcp and C^{270} in ASBT/Asbt to be the major site where inhibition of bile acid transport activity by thiol reagents is located. After site-directed mutagenesis of these cysteins to alanines, the carriers were almost insensitive toward thiophilic inactivation. However, they retained the full transport activity (Hallén et al. 2000; Saeki et al. 2002; Zahner et al. 2003; Banerjee et al. 2005). Therefore, it was concluded that C^{266}/C^{270} is not essential for bile acid transport of NTCP and ASBT by itself, but is located within or near the bile acid-binding pocket of these carriers. In contrast, several other cysteine–alanine or cysteine–threonine mutations abolished or highly reduced bile acid transport activity (i.e. C^{51}, C^{74}, C^{105}, C^{106}, C^{132}, C^{144} and C^{255} in ASBT/Asbt, as well as C^{96}, C^{98} and C^{250} in NTCP/Ntcp), indicating that these cysteines are required for transport function of the carriers (see Table 4). Furthermore, several mutations and polymorphisms were identified in human ASBT and NTCP, which dramatically reduced or even abolished bile acid transport function; i.e. L243P, T262M and P290S in ASBT, as well as I223T, S267F, I279T and K314E in NTCP (Wong et al. 1995; Oelkers et al. 1997; Ho et al. 2004). Most of the mentioned mutations affect amino acids that are highly conserved among NTCP/Ntcp, ASBT/Asbt and SOAT/Soat sequences (e.g. $C^{44,51}$, $C^{98,105}$, $C^{125,132}$,

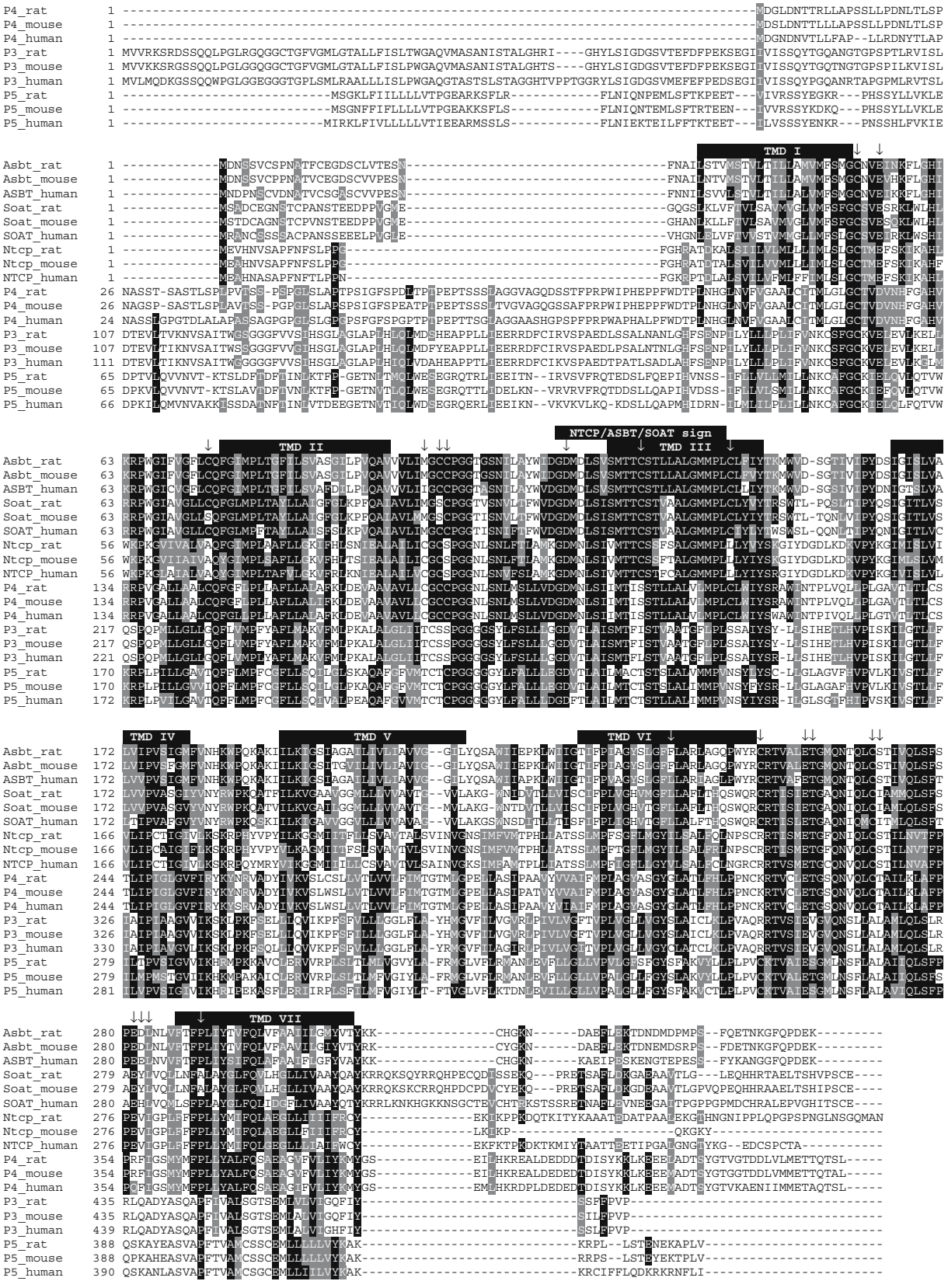

Fig. 3 Multiple alignment of human, rat, and mouse SLC10 family members. Deduced amino acid sequences were aligned using EBI *ClustalW* algorithm and alignment was visualised by BOXSHADE 3.21. Amino acid identity is displayed with *black* shading, while amino acid similarities are highlighted in *grey*. Positions of the respective amino acid residues are listed for each individual protein. Predictive localisation of the transmembrane domains (TMDs) is indicated. Only a seven-TMD topology is depicted. Amino acid residues, which were shown to be essential for transport function of the NTCP and ASBT, are marked by *arrows*. See text and Table 4 for further explanations

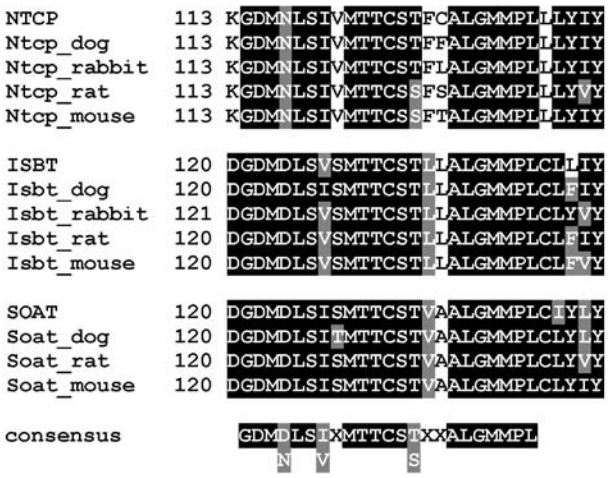

Fig. 4 NTCP/ASBT/SOAT signature motif. Deduced amino acid sequences were aligned using EBI *ClustalW* algorithm and alignment was visualised by BOXSHADE 3.21. Positions of the respective amino acid residues are listed for each individual protein. Human proteins are given in *capitals*; animal proteins are in *small letters* and are appended by the species name. The consensus sequence contains amino acids that are identical (*black* shading) or similar (*grey* shading) among all proteins. *X* represents significant differences within the protein alignment

$C^{250,255}$, $E^{257,261}$, $T^{258,262}$, $S^{267,271}$ and $P^{286,290}$; see Table 4 for further details). Given these data, absence of bile acid transport function of SOAT cannot be related to one of these amino acid residues. Vice versa, these amino acids cannot be directly involved in specific ligand binding on NTCP and ASBT, but may well affect essential protein structures and folding requirements.

Using a computer-generated 3D structure model of human ASBT, Zhang and coworkers suggested a putative ligand-binding site for bile acids to the surface structure of human ASBT (Zhang et al. 2004). The model identified E^{282} and L^{283} to be involved in the formation of dynamic hydrogen bonds with the 12α-hydroxy group of the bile acid, whereas residues in the vicinity of N^2 were capable of forming dynamic hydrogen bonds with either the 3α- or the 7α-hydroxy group of the bile acid (Zhang et al. 2004). However, this in silico-generated model does not fit exactly with experimental data concerning the 3D QSAR pharmacophore of ASBT (Bahringhaus et al. 1999) and the localisation of the bile acid-binding site of rabbit Asbt (Kramer et al. 2001a,b). In contrast to this in silico model, Kramer and coworkers localised the ligand binding site experimentally with a photoaffinity labelling approach using a 7,7-azo-bile acid derivative. In their experiments, the attachment site of the 7–OH group of the bile acid was addressed to the 67–56 C-terminal amino acids downstream of position 280 or 291 of rabbit Asbt. This region comprises the last transmembrane domain and the cytoplasmatic C-terminus. Further domains that could be involved in bile acid binding by Asbt could not be acquired with this approach (Kramer et al. 2001a,b). Interestingly, an alternatively spliced isoform of mouse Ntcp (Ntcp2) lacks the last 45 amino acid residues of the full-length mouse Ntcp1, but shows full sodium-dependent transport of bile acids when expressed in *Xenopus laevis* oocytes. This data suggests that even these C-terminal amino acids are not important for bile acid transport in Ntcp (Cattori et al. 1999).

Further structure–activity relationships of NTCP/Ntcp and ASBT/Asbt were addressed to the site of interaction with sodium ions, which are the principal cosubstrate of these carriers. As two sodium ions are translocated together with one bile acid molecule via NTCP and ASBT, this transport is electrogenic (Hagenbuch and Meier 1996; Weinman 1997; Weinman et al. 1998). As reported for other sodium-coupled cotransporters and exchangers (Nicoll et al. 1996; Jung 2001; Murtazina et al. 2001), negatively charged amino acids at the outer surface of the carrier protein are potential binding sites for cationic sodium ions. To address this question for rat Ntcp, a series of aspartate–asparagine and glutamate–glutamine mutations were screened for transport function and membrane expression in our group (Zahner et al. 2003). Three of the tested mutants were transport negative for bile acids: D24N, D115N and E257Q. D^{115} and E^{257} are highly conserved in all NTCP/Ntcp, ASBT/Asbt and SOAT/Soat sequences and are localised in the extracellular loops 1 (D^{115}) and 3 (E^{257}), indicating that these amino acids would be candidates for the extracellular sodium sensor for the Na^+/substrate cotransport. A further candidate with this function is E^{282} in human ASBT, since E282A and E282K mutations abolished taurocholate uptake, whereas E282D mutation recovered bile acid transport function (Zhang et al. 2004). However, E^{282} is not present in any other Asbt, NTCP/Ntcp or SOAT/Soat sequence.

After binding of the sodium ion to D^{115} and/or E^{257}, it has to be translocated through the pore-forming transmembrane helices to the cytoplasmic region of the carrier protein. Thereby, extracellular loops 1 and 3 could slide between the transmembrane domains into the membrane while forming a P-loop structure (see Fig. 5). Such a mechanism would allow the introduction of charged molecules into the inner part of the cell membrane, from where they can be released into the intracellular compartment (Zahner et al. 2003). This P-loop-based transport mechanism could also resolve the conflicting results from ASBT/NTCP topology predictions regarding the true number of transmembrane domains, i.e., two P-loop structures could fold as lipid-buried re-entrant loops in the plasma membrane but would not cross the membrane like a transmembrane domain (Hallén et al. 2002b). According to this transport mechanism, Na^+/bile acid cotransport by NTCP and ASBT would be the result of a series of ligand-induced conformational changes in the carrier proteins.

Phylogenetic relationships and evolutionary origin of the SLC10 family

To study the evolutionary origin of the SLC10 genes, a phylogenetic approach based on Bayesian inference was

Table 4 Mutations and polymorphisms in NTCP/Ntcp and ASBT/Asbt sequences that were shown to affect transport activity and/or expression: ↓ decrease, ↑ increase, ↔ no change, ∅ loss of function/expression. Highly conserved amino acid residues are in *bold*. ASBT/NTCP, human carriers; mNtcp/mAsbt, mouse carriers; rNtcp, rat carrier; IL, intracellular loop; EL, extracellular loop; TMD, transmembrane domain

Topology	NTCP/Ntcp	ASBT/Asbt	SOAT/Soat	Mutation / polymorphism	Transporter / species	Changes in transport activity, Km value (substrate)	Changes in membrane expression	Reference
IL1	**C^{44}**	**C^{51}**	**C^{51}**	C51A	ASBT	↓↓	↔	Banerjee et al. 2005,
				C51T	ASBT	∅	↔	Saeki et al. 2002,
				C51A	mAsbt	↓↓	↔	Zahner et al. 2003
				C44A	mNtcp	↔	↔	
				C44A	rNtcp	↔		
				C44W	rNtcp	↓		
	E^{47}	**E^{54}**	**E^{54}**	E47Q	rNtcp	↔		Zahner et al. 2003
	A^{67}	C^{74}	C/S^{74}	C74A	ASBT	∅	↓	Banerjee et al. 2005,
				C74T	ASBT	∅	∅	Saeki et al. 2002
				C74A	mAsbt	↓	↔	
EL1	C^{96}	M/I^{103}	M^{103}	C96A	mNtcp	∅	↔	Saeki et al. 2002,
				C96A	rNtcp	↔		Zahner et al. 2003
				C96W	rNtcp	↓↓		
	C^{98}	**C^{105}**	**S/C^{105}**	C105A	ASBT	∅	↔	Banerjee et al. 2005,
				C105T	ASBT	∅	↔	Saeki et al. 2002,
				C105A	mAsbt	↓	↔	Zahner et al. 2003
				C98A	mNtcp	↑	↔	
				C98A	rNtcp	↔		
				C98W	rNtcp	∅		
	S^{99}	**C^{106}**	**C^{106}**	C106A	ASBT	↓ 7.3 μM (TC)[b]	↔	Banerjee et al. 2005,
				C106T	ASBT	↓↓	↔	Saeki et al. 2002
				C106A	mAsbt	∅	↓	
	D^{115}	**D^{122}**	**D^{122}**	D115N	rNtcp	↓↓	↔	Zahner et al. 2003
TMD3	**C^{125}**	**C^{132}**	**C^{132}**	C132A	ASBT	↓↓	↔	Banerjee et al. 2005,
				C132T	ASBT	↓↓	↔	Saeki et al. 2002,
				C132A	mAsbt	↔	↔	Zahner et al. 2003
				C125A	mNtcp	↔	↔	
				C125A	rNtcp	↔		
	L^{137}	**C^{144}**	**C^{144}**	C144A	ASBT	∅	↓	Banerjee et al. 2005,
				C144T	ASBT	↔	↔	Saeki et al. 2002
				C144A	mAsbt	↓	↔	
IL3	L/I^{223}	W^{227}	L^{227}	I223T	NTCP*3	↓ 6.8 μM (TC)[a] ↓ 21 μM (C)[a] ↓↓ 19 μM (E_1S)[a]	↓↓	Ho et al. 2004
TMD6	I/V^{239}	F/L^{243}	L^{243}	L243P	ASBT	∅	↔	Oelkers et al. 1997
EL3	**C^{250}**	**C^{255}**	**C^{255}**	C255A	ASBT	↓↓	↔	Banerjee et al. 2005,
				C255T	ASBT	↓↓	↔	Saeki et al. 2002
				C255A	mAsbt	↔	↔	
				C250A	mNtcp	↓↓	↔	
	E^{257}	**E^{261}**	**E^{261}**	E257Q	rNtcp	∅	↔	Zahner et al. 2003
	T^{258}	**T^{262}**	**T^{262}**	T262M	ASBT	∅	↔	Oelkers et al. 1997
	C^{266}	**C^{270}**	**C^{270}**	C270A	ASBT	↔ 17 μM (TC)[b]	↔	Banerjee et al. 2005,
				C270T	ASBT	↓↓	↔	Hallén et al. 2000,
				C266A	NTCP	↔ 11 μM (TC)[c]		Saeki et al. 2002,
				C270A	ASBT	↔ 6.1 μM (TC)[d]		Zahner et al. 2003
				C270A	mAsbt	↔	↔	

Table 4 (continued)

Topology	NTCP/ Ntcp	ASBT/ Asbt	SOAT/ Soat	Mutation / polymorphism	Transporter / species	Changes in transport activity, Km value (substrate)	Changes in membrane expression	Reference
				C266A	mNtcp	↓	↔	
				C266A	rNtcp	↓	↔	
	S^{267}	**S^{271}**	I^{271}	S267F	NTCP*2	↓↓ 35 μM (TC)[a] ↓↓ 49 μM (C)[a] ↔ 29 μM (E_1S)[a]	↔	Ho et al. 2004
	E^{277}	**E^{281}**	**E^{281}**	E281A	ASBT	↓ 20 μM (TC)[e]	↔	Zhang et al. 2004,
				E277Q	rNtcp	↔		Zahner et al. 2003
	V^{278}	D/E^{282}	Y/H^{282}	E282A	ASBT	∅	↔	Zhang et al. 2004
				E282K	ASBT	∅	↔	
				E282D	ASBT	↓ 12 μM (TC)[e]	↔	
	I^{279}	**L^{283}**	**L^{283}**	I279T	NTCP*4	↓ 13 μM (TC)[a] ↓ 17 μM (C)[a] ↓ 30 μM (E_1S)[a]	↔	Ho et al. 2004
TMD7	**P^{286}**	**P^{290}**	**A/P^{290}**	P290S	ASBT	∅	↔	Wong et al. 1995

[a]Reference K_m of the wild type carrier=7.5 μM (TC=taurocholate), 12 μM (C=cholate), and 27 μM (E_1S=oestrone-3-sulfate) (Ho et al. 2004)
[b]Reference K_m of the wild type carrier=11 μM (TC=taurocholate) (Banerjee et al. 2005)
[c]Reference K_m of the wild type carrier=8.5 μM (TC=taurocholate) (Hallén et al. 2000)
[d]Reference K_m of the wild type carrier=8.3 μM (TC=taurocholate) (Hallén et al. 2000)
[e]Reference K_m of the wild type carrier=11 μM (TC=taurocholate) (Zhang et al. 2004)

applied using several mammalian and non-mammalian SLC10 sequences (i.e. from frog, fugu, zebrafish, dog, cattle, chimp, rat, mouse, chicken, and human). As an outgroup, a sequence from *Drosophila melanogaster* was used, which has a high sequence similarity to the SLC10 family members. As shown in Fig. 6, the SLC10 family consists of two major clades. Major clade I comprises SOAT, ASBT, NTCP and P4 genes; major clade II contains P3 and P5 genes. Within clade I, SOAT is the sister group to ASBT and P4 is the sister to NTCP. Reflecting the relative time frame of these gene duplication events, which can be deduced from a lineage-through-time plot shown in Fig. 6, the split of SOAT and ASBT is significantly younger ($P<0.001$) than the split of NTCP and P4. This could explain the much higher sequence identity between ASBT and SOAT than between NTCP and P4.

Plotting the transport functions of SOAT, ASBT, NTCP and P4 to the emerging of the corresponding genes, it is surprising that, although these genes derived from a common ancestor gene, they clearly differ in their transport

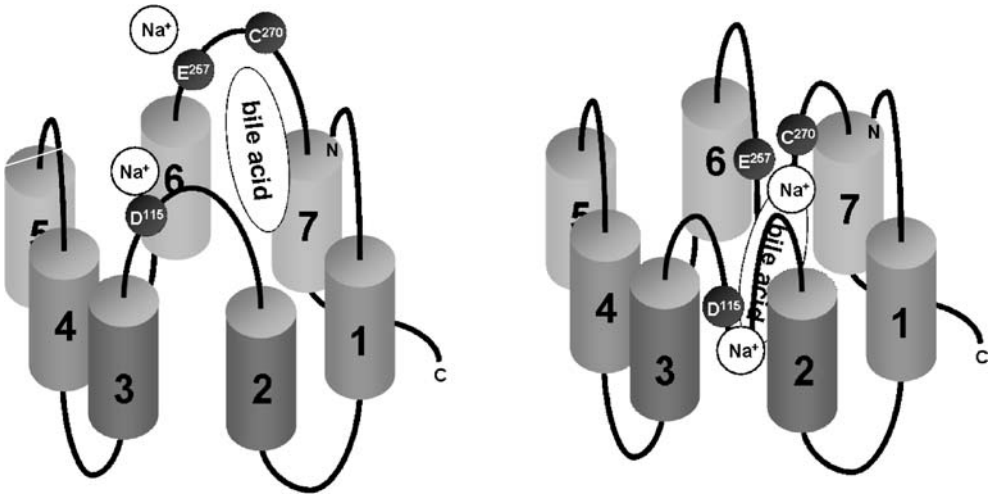

Fig. 5 P-loop model for rat Ntcp, modified from Zahner et al. (2003). After binding of the substrate and the sodium ions, extracellular loops 1 and 3 can slide into the membrane compartment forming a P-loop structure. From that, substrate and sodium ions can be released into the intracellular compartment. Sodium ions can bind to D^{115} and E^{257}, which are referred to as "sodium sensor" of the Na^+/substrate cotransport. Amino acids that are involved in substrate binding have not been exactly identified. Most likely, these are located in extracellular loop 3 and transmembrane domain 7 (see text for further explanations)

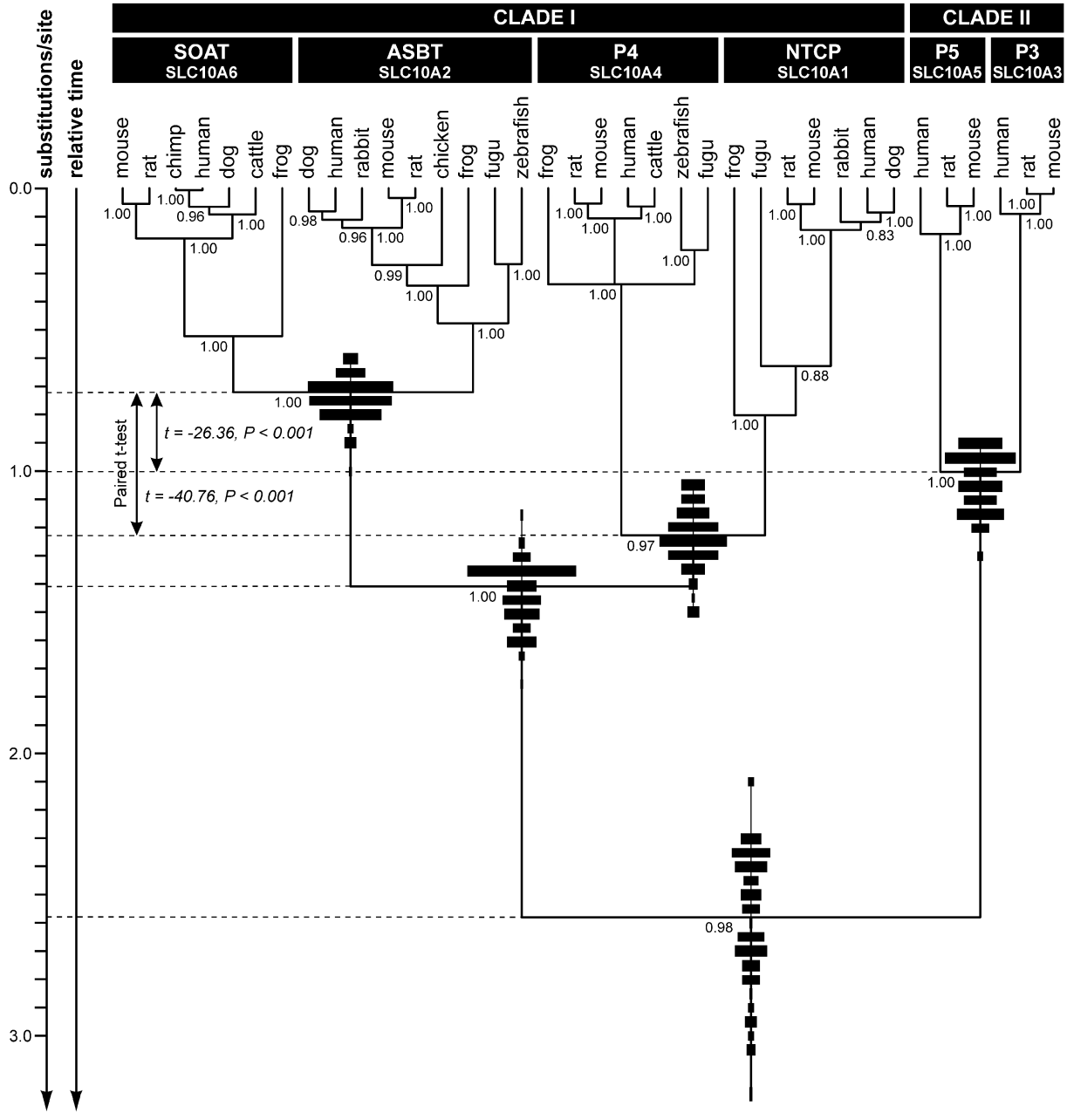

Fig. 6 Clock-enforced Bayesian cDNA tree with lineages-through-time plot of selected mammalian and non-mammalian members of the SLC10 family. Respective cDNA sequences were aligned with *ClustalW* and truncated to the shortest sequence, resulting in 864 aligned nucleotide positions. As outgroup, a *Drosophila* sequence with high sequence similarity to the SLC10 family members was used. Phylogenetic reconstruction was performed in MrBayes 3.1 (Ronquist and Huelsenbeck 2003) based on the best-fit model of sequence evolution (TvN with invariable sites and Γ-distribution) suggested by the Akaike Information Criterion implemented in Modeltest 3.6 (Posada and Crandall 1998). A total of 1,000,000 generations was sampled with the current tree saved at intervals of 10 generations. The 50% majority rule tree shown here was constructed from all sampled trees, with the first 1,000 trees (10,000 generations) ignored as burn-in. All major clades (i.e. protein subfamilies) are resolved with posterior probabilities greater than 0.95 (plotted at nodes). Vertical branch lengths reflect the substitutions per site (see scale on the left). In a clock-enforced tree, they also reflect coalescent time. However, as no clock rate is known for the SLC family, absolute times cannot be provided. In order to test whether SOAT and ASBT represent the youngest members of the SLC10 family shown here, the variance of the node depths of selected splits was calculated for the 100 best trees from the Bayesian search. The frequency distributions for the node depths are given for each major clade. Pairwise comparisons of node depths in the 100 best trees for the split of SOAT/ASBT on the one side and P4/NTCP and P5/P3 on the other side using paired *t*-tests indicated that the depth of the nodes (and therefore their age) differs significantly between both SOAT/ASBT and P4/NTCP as well as between SOAT/ASBT and P5/P3. It therefore can be assumed that the split of SOAT and ASBT is the youngest split among SLC10 subfamilies included in the present study

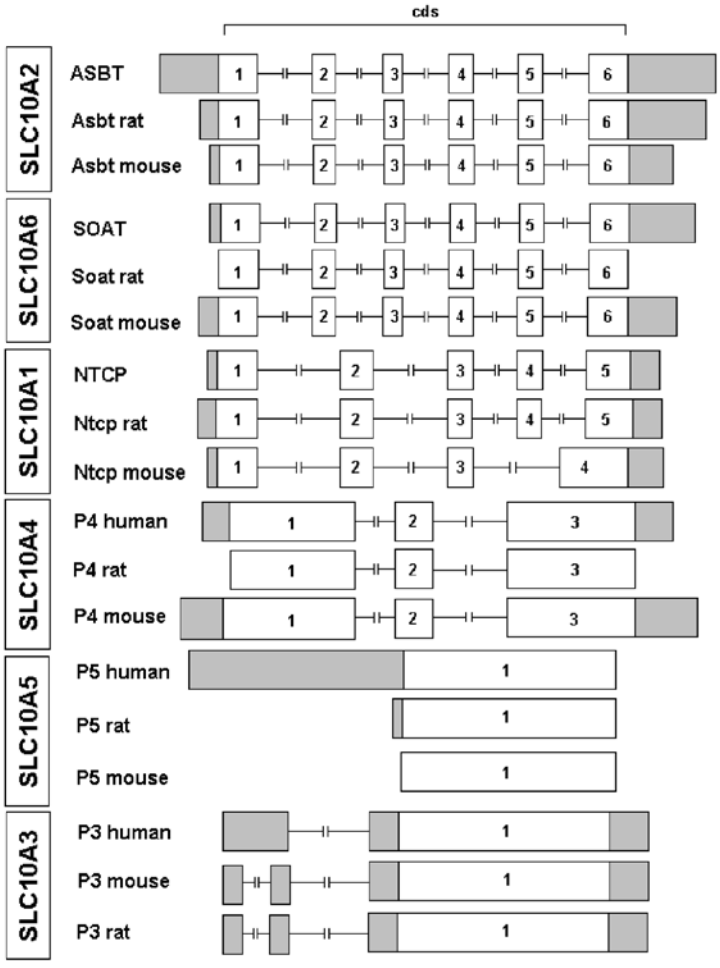

Chrom.	Gene (kb)	Protein (aa)
13q33	22.8	348
16q12	22.2	348
8 A1	19.6	348
4q21	25.4	377
14p22	21.3	370
5 E5	23.7	373
14q24	21.4	349
6q24	13.6	362
12 D1	12.5	362
4p12	5.72	437
14p11	5.22	437
5 C3	6.05	437
8q21	2.52	438
2q23	1.33	434
3 A1	1.31	434
Xq28	3.35	477
X A7	4.04	473
Xq37	3.87	473

Fig. 7 Exon/intron structure of the SLC10/Slc10 genes. Exons are represented by *boxes* and introns by *broken lines*. Untranslated regions flanking the coding sequence (*cds*) are *shaded*. Chromosomal localisation and lengths of the genes and coded proteins are indicated

functions. The most parsimonious explanation would be that the ancestor of clade I incorporated both functional properties, i.e., transport of bile acids and steroid sulfates. During further subdivision into ASBT and SOAT, the transport function separated: ASBT kept bile acid transport and SOAT, steroid sulfate transport. In contrast, during the subdivision into NTCP and P4, NTCP retained transport functions for both kind of substrates, whereas P4 lost both of them. Whether P4 is a transporter for another kind of substrate is unknown. The fact that P4 is highly conserved in several mammalian and non-mammalian species and its expression is dominant in nervous tissue may indicate some (unknown) physiological importance.

Genomic organisation of the SLC10 genes

The results of the phylogenetic analyses are in good concordance with the genomic organisation of the SLC10 genes. SOAT and ASBT genes are most closely related not only phylogenetically, but also in their gene structures. Both genes exhibit six coding exons for all species, with highly conserved exon/intron boundaries and identical exon lengths (Fig. 7). However, the two genes do not share a common gene locus: the ASBT/Asbt genes are on chromosomes 13, 16 and 8 and the SOAT/Soat genes on chromosomes 4, 14 and 5 in man, rat and mouse, respectively. In contrast, gene structure and protein length of NTCP and P4 have fewer similarities, which could be explained by the longer history of separated gene development than for ASBT and SOAT genes. P3 and P5 genes have only one coding exon and accordingly a much smaller gene size. However, the less complex genes of P3, P4 and P5 are coding for much longer proteins (437–477 amino acids) compared to NTCP, ASBT and SOAT (348–377 amino acids). Whether or not these differences are important for the functional properties of the individual SLC10 proteins has to be further elucidated.

References

Adachi J, Waddell PJ, Martin W, Hasegawa M (2000) Plastid genome phylogeny and a model of amino acid substitution for proteins encoded by chloroplast DNA. J Mol Evol 50:348–358

Alcalay M, Toniolo D (1988) CpG islands of the X chromosome are gene associated. Nucleic Acids Res 16:9527–9543

Alpini G, Glaser SS, Rodgers R, Phinizy JL, Robertson WE, Lasater J, Caligiuri A, Tretjak Z, LeSage GD (1997) Functional expression of the apical Na^+-dependent bile acid transporter in large but not small rat cholangiocytes. Gastroenterology 113:1734–1740

Ananthanarayanan M, Ng OC, Boyer JL, Suchy FJ (1994) Characterization of cloned rat liver Na^+-bile acid cotransporter using peptide and fusion protein antibodies. Am J Physiol 267: G637–G643

Anwer MS (2004) Cellular regulation of hepatic bile acid transport in health and cholestasis. Hepatology 39(3):581–590

Anwer MS, Gillin H, Mukhopadhyay S, Balasubramaniyan N, Suchy FJ, Ananthanarayanan M (2005) Dephosphorylation of Ser-226 facilitates plasma membrane retention of Ntcp. J Biol Chem 280:33687–33692

Arrese M, Trauner M, Sacchiero RJ, Crossman MW, Shneider BL (1998) Neither intestinal sequestration of bile acids nor common bile duct ligation modulate the expression and function of the rat ileal bile acid transporter. Hepatology 28:1081–1087

Banerjee A, Ray A, Chang C, Swaan PW (2005) Site-directed mutagenesis and use of bile acid-MTS conjugates to probe the role of cysteines in the human apical sodium-dependent bile acid transporter (SLC10A2). Biochemistry 44:8908–8917

Baringhaus KH, Matter H, Stengelin S, Kramer W (1999) Substrate specificity of the ileal and the hepatic Na^+/bile acid cotransporters of the rabbit. II. A reliable 3D QSAR pharmacophore model for the ileal Na^+/bile acid cotransporter. J Lipid Res 40:2158–2168

Baulieu EE (1996) Dehydroepiandrosterone (DHEA): a fountain of youth? J Clin Endocrinol Metab 81:3147–3151

Bhat BG, Rapp SR, Beaudry JA, Napawan N, Butteiger DN, Hall KA, Null CL, Luo Y, Keller BT (2003) Inhibition of ileal bile acid transport and reduced atherosclerosis in apoE-/- mice by SC-435. J Lipid Res 44:1614–1621

Bjorkhem I, Lund E, Rudling M (1997) Coordinate regulation of cholesterol 7 alpha-hydroxylase and HMG-CoA reductase in the liver. Subcell Biochem 28:23–55

Blumrich M, Petzinger E (1990) Membrane transport of conjugated and unconjugated bile acids into hepatocytes is susceptible to SH-blocking reagents. Biochim Biophys Acta 1029:1–12

Blumrich M, Petzinger E (1993) Two distinct types of SH-groups are necessary for bumetanide and bile acid uptake into isolated rat hepatocytes. Biochim Biophys Acta 1149:278–284

Boyer JL, Ng OC, Ananthanarayanan M, Hofmann AF, Schteingart CD, Hagenbuch B, Stieger B, Meier PJ (1994) Expression and characterization of a functional rat liver Na^+ bile acid cotransport system in COS-7 cells. Am J Physiol 266: G382–G387

Cattori V, Eckhardt U, Hagenbuch B (1999) Molecular cloning and functional characterization of two alternatively spliced Ntcp isoforms from mouse liver. Biochim Biophys Acta 1445: 154–159

Chen F, Ma L, Dawson PA, Sinal CJ, Sehayek E, Gonzalez FJ, Breslow J, Ananthanarayanan M, Shneider BL (2003) Liver receptor homologue-1 mediates species- and cell line-specific bile acid-dependent negative feedback regulation of the apical sodium-dependent bile acid transporter. J Biol Chem 278:19909–19916

Chiang JY, Kimmel R, Weinberger C, Stroup D (2000) Farnesoid X receptor responds to bile acids and represses cholesterol 7alpha-hydroxylase gene (CYP7A1) transcription. J Biol Chem 275:10918–10924

Christie DM, Dawson PA, Thevananther S, Shneider BL (1996) Comparative analysis of the ontogeny of a sodium-dependent bile acid transporter in rat kidney and ileum. Am J Physiol 271: G377–G385

Cohn MA, Rounds DJ, Karpen SJ, Ananthanarayanan M, Suchy FJ (1995) Assignment of a rat liver Na^+/bile acid cotransporter gene to chromosome 6q24. Mamm Genome 6:60

Craddock AL, Love MW, Daniel RW, Kirby LC, Walters HC, Wong MH, Dawson PA (1998) Expression and transport properties of the human ileal and renal sodium-dependent bile acid transporter. Am J Physiol 274:G157–G169

Dawson PA, Oelkers P (1995) Bile acid transporters. Curr Opin Lipidol 6:109–114

Dawson PA, Haywood J, Craddock AL, Wilson M, Tietjen M, Kluckman K, Maeda N, Parks JS (2003) Targeted deletion of the ileal bile acid transporter eliminates enterohepatic cycling of bile acids in mice. J Biol Chem 278:33920–33927

Dietschy JM, Turley SD, Spady DK (1993) Role of liver in the maintenance of cholesterol and low density lipoprotein homeostasis in different animal species, including humans. J Lipid Res 34:1637–1659

Dranoff JA, McClure M, Burgstahler AD, Denson LA, Crawford AR, Crawford JM, Karpen SJ, Nathanson MH (1999) Short-term regulation of bile acid uptake by microfilament-dependent translocation of rat ntcp to the plasma membrane. Hepatology 30:223–229

Gardiner-Garden M, Frommer M (1987) CpG islands in vertebrate genomes. J Mol Biol 196:261–282

Geyer J, Godoy JR, Petzinger E (2004) Identification of a sodium-dependent organic anion transporter from rat adrenal gland. Biochem Biophys Res Commun 316:300–306

Green RM, Ananthanarayanan M, Suchy FJ, Beier DR (1998) Genetic mapping of the Na^+-taurocholate cotransporting polypeptide to mouse chromosome 12. Mamm Genome 9:598

Hagenbuch B (1997) Molecular properties of hepatic uptake systems for bile acids and organic anions. J Membr Biol 160:1–8

Hagenbuch B, Dawson P (2004) The sodium bile salt cotransport family SLC10. Pflügers Arch 447:566–570

Hagenbuch B, Meier PJ (1994) Molecular cloning, chromosomal localization, and functional characterization of a human liver Na^+/bile acid cotransporter. J Clin Invest 93:1326–1331

Hagenbuch B, Meier PJ (1996) Sinusoidal (basolateral) bile salt uptake systems of hepatocytes. Semin Liver Dis 16:129–136

Hagenbuch B, Lubbert H, Stieger B, Meier PJ (1990) Expression of the hepatocyte Na^+/bile acid cotransporter in *Xenopus laevis* oocytes. J Biol Chem 265:5357–5360

Hagenbuch B, Stieger B, Foguet M, Lubbert H, Meier PJ (1991) Functional expression cloning and characterization of the hepatocyte Na^+/bile acid cotransport system. Proc Natl Acad Sci U S A 88:10629–10633

Hagenbuch B, Scharschmidt BF, Meier PJ (1996) Effect of antisense oligonucleotides on the expression of hepatocellular bile acid and organic anion uptake systems in *Xenopus laevis* oocytes. Biochem J 316(Pt 3):901–904

Hall TA (1999) BioEdit: a user-friendly biological sequence alignment editor and analysis program for Windows 95/98/NT. Nucl Acids Symp Ser 41:95–98

Hallén S, Branden M, Dawson PA, Sachs G (1999) Membrane insertion scanning of the human ileal sodium/bile acid cotransporter. Biochemistry 38:11379–11388

Hallén S, Fryklund J, Sachs G (2000) Inhibition of the human sodium/bile acid cotransporters by side-specific methanethiosulfonate sulfhydryl reagents: substrate-controlled accessibility of site of inactivation. Biochemistry 39:6743–6750

Hallén S, Bjorquist A, Ostlund-Lindqvist AM, Sachs G (2002a) Identification of a region of the ileal-type sodium/bile acid cotransporter interacting with a competitive bile acid transport inhibitor. Biochemistry 41:14916–14924

Hallén S, Mareninova O, Branden M, Sachs G (2002b) Organization of the membrane domain of the human liver sodium/bile acid cotransporter. Biochemistry 41:7253–7266

Hara S, Higaki J, Higashino K, Iwai M, Takasu N, Miyata K, Tonda K, Nagata K, Goh Y, Mizui T (1997) S-8921, an ileal Na^+/bile acid cotransporter inhibitor decreases serum cholesterol in hamsters. Life Sci 60:365–370

Hata S, Wang P, Eftychiou N, Ananthanarayanan M, Batta A, Salen G, Pang KS, Wolkoff AW (2003) Substrate specificities of rat oatp1 and ntcp: implications for hepatic organic anion uptake. Am J Physiol Gastrointest Liver Physiol 285:G829–G839

Hediger MA, Romero MF, Peng JB, Rolfs A, Takanaga H, Bruford EA (2004) The ABCs of solute carriers: physiological, pathological and therapeutic implications of human membrane transport proteins. Introduction. Pflügers Arch 447:465–468

Higaki J, Hara S, Takasu N, Tonda K, Miyata K, Shike T, Nagata K, Mizui T (1998) Inhibition of ileal Na^+/bile acid cotransporter by S-8921 reduces serum cholesterol and prevents atherosclerosis in rabbits. Arterioscler Thromb Vasc Biol 18:1304–1311

Ho RH, Leake BF, Roberts RL, Lee W, Kim RB (2004) Ethnicity-dependent polymorphism in Na^+-taurocholate cotransporting polypeptide (SLC10A1) reveals a domain critical for bile acid substrate recognition. J Biol Chem 279:7213–7222

Howarth NM, Purohit A, Robinson JJ, Vicker N, Reed MJ, Potter BV (2002) Estrone 3-sulfate mimics inhibitors of estrone sulfatase activity: homology model construction and docking studies. Biochemistry 41:14801–14814

Huang HC, Tremont SJ, Lee LF, Keller BT, Carpenter AJ, Wang CC, Banerjee SC, Both SR, Fletcher T, Garland DJ, Huang W, Jones C, Koeller KJ, Kolodziej SA, Li J, Manning RE, Mahoney MW, Miller RE, Mischke DA, Rath NP, Reinhard EJ, Tollefson MB, Vernier WF, Wagner GM, Rapp SR, Beaudry J, Glenn K, Regina K, Schuh JR, Smith ME, Trivedi JS, Reitz DB (2005) Discovery of potent, nonsystemic apical sodium-codependent bile acid transporter inhibitors (Part 2). J Med Chem 48:5853–5868

Huelsenbeck J, Rannala B (2004) Frequentist properties of Bayesian posterior probabilities of phylogenetic trees under simple and complex substitution models. Syst Biol 53:904–913

Huff MW, Telford DE, Edwards JY, Burnett JR, Barrett PH, Rapp SR, Napawan N, Keller BT (2002) Inhibition of the apical sodium-dependent bile acid transporter reduces LDL cholesterol and apoB by enhanced plasma clearance of LDL apoB. Arterioscler Thromb Vasc Biol 22:1884–1891

Ichihashi T, Izawa M, Miyata K, Mizui T, Hirano K, Takagishi Y (1998) Mechanism of hypocholesterolemic action of S-8921 in rats: S-8921 inhibits ileal bile acid absorption. J Pharmacol Exp Ther 284:43–50

Jung H (2001) Towards the molecular mechanism of Na^+/solute symport in prokaryotes. Biochim Biophys Acta 1505:131–143

Kim RB, Leake B, Cvetkovic M, Roden MM, Nadeau J, Walubo A, Wilkinson GR (1999) Modulation by drugs of human hepatic sodium-dependent bile acid transporter (sodium taurocholate cotransporting polypeptide) activity. J Pharmacol Exp Ther 291:1204–1209

Kim JY, Kim KH, Lee JA, Namkung W, Sun AQ, Ananthanarayanan M, Suchy FJ, Shin DM, Muallem S, Lee MG (2002) Transporter-mediated bile acid uptake causes Ca^{2+}-dependent cell death in rat pancreatic acinar cells. Gastroenterology 122:1941–1953

Kramer W, Wess G (1996) Bile acid transport systems as pharmaceutical targets. Eur J Clin Invest 26:715–732

Kramer W, Nicol SB, Girbig F, Gutjahr U, Kowalewski S, Fasold H (1992) Characterization and chemical modification of the Na^+-dependent bile-acid transport system in brush-border membrane vesicles from rabbit ileum. Biochim Biophys Acta 1111:93–102

Kramer W, Wess G, Bewersdorf U, Corsiero D, Girbig F, Weyland C, Stengelin S, Enhsen A, Bock K, Kleine H, Le Dreau MA, Schafer HL (1997) Topological photoaffinity labeling of the rabbit ileal Na^+/bile-salt-cotransport system. Eur J Biochem 249:456–464

Kramer W, Stengelin S, Baringhaus KH, Enhsen A, Heuer H, Becker W, Corsiero D, Girbig F, Noll R, Weyland C (1999) Substrate specificity of the ileal and the hepatic Na^+/bile acid cotransporters of the rabbit. I. Transport studies with membrane vesicles and cell lines expressing the cloned transporters. J Lipid Res 40:1604–1617

Kramer W, Girbig F, Glombik H, Corsiero D, Stengelin S, Weyland C (2001a) Identification of a ligand-binding site in the Na^+/bile acid cotransporting protein from rabbit ileum. J Biol Chem 276:36020–36027

Kramer W, Sauber K, Baringhaus KH, Kurz M, Stengelin S, Lange G, Corsiero D, Girbig F, Konig W, Weyland C (2001b) Identification of the bile acid-binding site of the ileal lipid-binding protein by photoaffinity labeling, matrix-assisted laser desorption ionization-mass spectrometry, and NMR structure. J Biol Chem 276:7291–7301

Kullak-Ublick GA, Glasa J, Boker C, Oswald M, Grutzner U, Hagenbuch B, Stieger B, Meier PJ, Beuers U, Kramer W, Wess G, Paumgartner G (1997) Chlorambucil-taurocholate is transported by bile acid carriers expressed in human hepatocellular carcinomas. Gastroenterology 113:1295–1305

Kullak-Ublick GA, Stieger B, Hagenbuch B, Meier PJ (2000a) Hepatic transport of bile salts. Semin Liver Dis 20:273–292

Kullak-Ublick GA, Ismair MG, Kubitz R, Schmitt M, Häussinger D, Stieger B, Hagenbuch B, Meier PJ, Beuers U, Paumgartner G (2000b) Stable expression and functional characterization of a Na^+-taurocholate cotransporting green fluorescent protein in human hepatoblastoma HepG2 cells. Cytotech 34:1–9

Kullak-Ublick GA, Stieger B, Meier PJ (2004) Enterohepatic bile salt transporters in normal physiology and liver disease. Gastroenterology 126:322–342

Kurata H, Suzuki S, Ohhata Y, Ikeda T, Hasegawa T, Kitayama K, Inaba T, Kono K, Kohama T (2004) A novel class of apical sodium-dependent bile acid transporter inhibitors: the amphiphilic 4-oxo-1-phenyl-1,4-dihydroquinoline derivatives. Bioorg Med Chem Lett 14:1183–1186

Labrie F, Belanger A, Luu-The V, Labrie C, Simard J, Cusan L, Gomez JL, Candas B (1998) DHEA and the intracrine formation of androgens and estrogens in peripheral target tissues: its role during aging. Steroids 63:322–328

Lazaridis KN, Pham L, Tietz P, Marinelli RA, deGroen PC, Levine S, Dawson PA, LaRusso NF (1997) Rat cholangiocytes absorb bile acids at their apical domain via the ileal sodium-dependent bile acid transporter. J Clin Invest 100:2714–2721

Lazaridis KN, Tietz P, Wu T, Kip S, Dawson PA, LaRusso NF (2000) Alternative splicing of the rat sodium/bile acid transporter changes its cellular localization and transport properties. Proc Natl Acad Sci U S A 97:11092–11097

Lewis MC, Brieaddy LE, Root C (1995) Effects of 2164U90 on ileal bile acid absorption and serum cholesterol in rats and mice. J Lipid Res 36:1098–1105

Li H, Xu G, Shang Q, Pan L, Shefer S, Batta AK, Bollineni J, Tint GS, Keller BT, Salen G (2004) Inhibition of ileal bile acid transport lowers plasma cholesterol levels by inactivating hepatic farnesoid X receptor and stimulating cholesterol 7 alpha-hydroxylase. Metabolism 53:927–932

Li H, Chen F, Shang Q, Pan L, Shneider BL, Chiang JY, Forman BM, Ananthanarayanan M, Tint GS, Salen G, Xu G (2005) FXR-activating ligands inhibit rabbit ASBT expression via FXR-SHP-FTF cascade. Am J Physiol Gastrointest Liver Physiol 288:G60–G66

Marin JJG, Romero MR, Vallejo M, Perez MJ, Briz O (2005) Emerging interest in bile acid transporters in pathophysiology and pharmacology. Med Hypotheses Res 2:425–448

Meier PJ, Stieger B (2002) Bile salt transporters. Annu Rev Physiol 64:635–661

Meier PJ, Eckhardt U, Schroeder A, Hagenbuch B, Stieger B (1997) Substrate specificity of sinusoidal bile acid and organic anion uptake systems in rat and human liver. Hepatology 26: 1667–1677

Mukhopadhayay S, Ananthanarayanan M, Stieger B, Meier PJ, Suchy FJ, Anwer MS (1997) cAMP increases liver Na^+-taurocholate cotransport by translocating transporter to plasma membranes. Am J Physiol 273:G842–G848

Murtazina R, Booth BJ, Bullis BL, Singh DN, Fliegel L (2001) Functional analysis of polar amino-acid residues in membrane associated regions of the NHE1 isoform of the mammalian Na^+/H^+ exchanger. Eur J Biochem 268:4674–4685

Neimark E, Chen F, Li X, Shneider BL (2004) Bile acid-induced negative feedback regulation of the human ileal bile acid transporter. Hepatology 40:149–156

Nicoll DA, Hryshko LV, Matsuoka S, Frank JS, Philipson KD (1996) Mutation of amino acid residues in the putative transmembrane segments of the cardiac sarcolemmal Na^+-Ca^{2+} exchanger. J Biol Chem 271:13385–13391

Oelkers P, Kirby LC, Heubi JE, Dawson PA (1997) Primary bile acid malabsorption caused by mutations in the ileal sodium-dependent bile acid transporter gene (SLC10A2). J Clin Invest 99:1880–1887

Platia MP, Fencl MD, Elkind-Hirsch KE, Canick JA, Tulchinsky D (1984) Estrone sulfatase activity in the human brain and estrone sulfate levels in the normal menstrual cycle. J Steroid Biochem 21:237–241

Platte HD, Honscha W, Schuh K, Petzinger E (1996) Functional characterization of the hepatic sodium-dependent taurocholate transporter stably transfected into an immortalized liver-derived cell line and V79 fibroblasts. Eur J Cell Biol 70:54–60

Posada D, Crandall KA (1998) MODELTEST: testing the model of DNA substitution. Bioinformatics 14:817–818

Ronquist F, Huelsenbeck JP (2003) MrBayes 3: Bayesian phylogenetic inference under mixed models. Bioinformatics 19: 1572–1574

Root C, Smith CD, Winegar DA, Brieaddy LE, Lewis MC (1995) Inhibition of ileal sodium-dependent bile acid transport by 2164U90. J Lipid Res 36:1106–1115

Root C, Smith CD, Sundseth SS, Pink HM, Wilson JG, Lewis MC (2002) Ileal bile acid transporter inhibition, CYP7A1 induction, and antilipemic action of 264W94. J Lipid Res 43:1320–1330

Saeki T, Matoba K, Furukawa H, Kirifuji K, Kanamoto R, Iwami K (1999) Characterization, cDNA cloning, and functional expression of mouse ileal sodium-dependent bile acid transporter. J Biochem (Tokyo) 125:846–851

Saeki T, Kuroda T, Matsumoto M, Kanamoto R, Iwami K (2002) Effects of Cys mutation on taurocholic acid transport by mouse ileal and hepatic sodium-dependent bile acid transporters. Biosci Biotechnol Biochem 66:467–470

Schroeder A, Eckhardt U, Stieger B, Tynes R, Schteingart CD, Hofmann AF, Meier PJ, Hagenbuch B (1998) Substrate specificity of the rat liver Na^+-bile salt cotransporter in *Xenopus laevis* oocytes and in CHO cells. Am J Physiol 274: G370–G375

Shih DQ, Bussen M, Sehayek E, Ananthanarayanan M, Shneider BL, Suchy FJ, Shefer S, Bollileni JS, Gonzalez FJ, Breslow JL, Stoffel M (2001) Hepatocyte nuclear factor-1alpha is an essential regulator of bile acid and plasma cholesterol metabolism. Nat Genet 27:375–382

Shneider BL (2001) Intestinal bile acid transport: biology, physiology, and pathophysiology. J Pediatr Gastroenterol Nutr 32: 407–417

Shneider BL, Dawson PA, Christie DM, Hardikar W, Wong MH, Suchy FJ (1995) Cloning and molecular characterization of the ontogeny of a rat ileal sodium-dependent bile acid transporter. J Clin Invest 95:745–754

Stengelin S, Apel S, Becker W, Maier M, Rosenberger J, Bewersdorf U, Girbig F, Weyland C, Wess G, Kramer W (1996) The rabbit ileal lipid-binding protein. Gene cloning and functional expression of the recombinant protein. Eur J Biochem 239:887–896

Stieger B, Hagenbuch B, Landmann L, Hochli M, Schroeder A, Meier PJ (1994) In situ localization of the hepatocytic Na^+/taurocholate cotransporting polypeptide in rat liver. Gastroenterology 107:1781–1787

Sun AQ, Ananthanarayanan M, Soroka CJ, Thevananther S, Shneider BL, Suchy FJ (1998) Sorting of rat liver and ileal sodium-dependent bile acid transporters in polarized epithelial cells. Am J Physiol 275:G1045–G1055

Sun AQ, Arrese MA, Zeng L, Swaby I, Zhou MM, Suchy FJ (2001) The rat liver Na^+/bile acid cotransporter. Importance of the cytoplasmic tail to function and plasma membrane targeting. J Biol Chem 276:6825–6833

Sun AQ, Salkar R, Sachchidanand, Xu S, Zeng L, Zhou MM, Suchy FJ (2003) A 14-amino acid sequence with a beta-turn structure is required for apical membrane sorting of the rat ileal bile acid transporter. J Biol Chem 278:4000–4009

Swaan PW, Szoka FC Jr, Oie S (1997) Molecular modeling of the intestinal bile acid carrier: a comparative molecular field analysis study. J Comput Aided Mol Des 11:581–588

Telford DE, Edwards JY, Lipson SM, Sutherland B, Barrett PH, Burnett JR, Krul ES, Keller BT, Huff MW (2003) Inhibition of both the apical sodium-dependent bile acid transporter and HMG-CoA reductase markedly enhances the clearance of LDL apoB. J Lipid Res 44:943–952

Tollefson MB, Vernier WF, Huang HC, Chen FP, Reinhard EJ, Beaudry J, Keller BT, Reitz DB (2000) A novel class of apical sodium co-dependent bile acid transporter inhibitors: the 2,3-disubstituted-4-phenylquinolines. Bioorg Med Chem Lett 10:277–279

Trauner M, Boyer JL (2003) Bile salt transporters: molecular characterization, function, and regulation. Physiol Rev 83: 633–671

Tremont SJ, Lee LF, Huang HC, Keller BT, Banerjee SC, Both SR, Carpenter AJ, Wang CC, Garland DJ, Huang W, Jones C, Koeller KJ, Kolodziej SA, Li J, Manning RE, Mahoney MW, Miller RE, Mischke DA, Rath NP, Fletcher T, Reinhard EJ, Tollefson MB, Vernier WF, Wagner GM, Rapp SR, Beaudry J, Glenn K, Regina K, Schuh JR, Smith ME, Trivedi JS, Reitz DB (2005) Discovery of potent, nonsystemic apical sodium-codependent bile acid transporter inhibitors (Part 1). J Med Chem 48:5837–5852

Vlahcevic ZR, Pandak WM, Stravitz RT (1999) Regulation of bile acid biosynthesis. Gastroenterol Clin North Am 28:1–25

Wagner M, Trauner M (2005) Transcriptional regulation of hepatobiliary transport systems in health and disease: implications for a rationale approach to the treatment of intrahepatic cholestasis. Ann Hepatol 4:77–99

Webster CR, Blanch C, Anwer MS (2002) Role of PP2B in cAMP-induced dephosphorylation and translocation of NTCP. Am J Physiol Gastrointest Liver Physiol 283:G44–G50

Weinman SA (1997) Electrogenicity of Na^+-coupled bile acid transporters. Yale J Biol Med 70:331–340

Weinman SA, Carruth MW, Dawson PA (1998) Bile acid uptake via the human apical sodium-bile acid cotransporter is electrogenic. J Biol Chem 273:34691–34695

Wess G, Kramer W, Enhsen A, Glombik H, Baringhaus KH, Boger G, Urmann M, Bock K, Kleine H, Neckermann G (1994) Specific inhibitors of ileal bile acid transport. J Med Chem 37:873–875

West KL, Ramjiganesh T, Roy S, Keller BT, Fernandez ML (2002) 1-[4-[4[(4R,5R)-3,3-Dibutyl-7-(dimethylamino)-2,3,4,5-tetrahydro-4-hydroxy -1,1-dioxido-1-benzothiepin-5-yl]phenoxy] butyl]-4-aza-1-azoniabicyclo[2.2. 2]octane methanesulfonate (SC-435), an ileal apical sodium-codependent bile acid transporter inhibitor alters hepatic cholesterol metabolism and lowers plasma low-density lipoprotein-cholesterol concentrations in guinea pigs. J Pharmacol Exp Ther 303:293–299

West KL, Zern TL, Butteiger DN, Keller BT, Fernandez ML (2003) SC-435, an ileal apical sodium co-dependent bile acid transporter (ASBT) inhibitor lowers plasma cholesterol and reduces atherosclerosis in guinea pigs. Atherosclerosis 171:201–210

Wong MH, Oelkers P, Craddock AL, Dawson PA (1994) Expression cloning and characterization of the hamster ileal sodium-dependent bile acid transporter. J Biol Chem 269:1340–1347

Wong MH, Oelkers P, Dawson PA (1995) Identification of a mutation in the ileal sodium-dependent bile acid transporter gene that abolishes transport activity. J Biol Chem 270: 27228–27234

Wong MH, Rao PN, Pettenati MJ, Dawson PA (1996) Localization of the ileal sodium-bile acid cotransporter gene (SLC10A2) to human chromosome 13q33. Genomics 33:538–540

Zahner D, Eckhardt U, Petzinger E (2003) Transport of taurocholate by mutants of negatively charged amino acids, cysteines, and threonines of the rat liver sodium-dependent taurocholate cotransporting polypeptide Ntcp. Eur J Biochem 270: 1117–1127

Zhang EY, Phelps MA, Banerjee A, Khantwal CM, Chang C, Helsper F, Swaan PW (2004) Topology scanning and putative three-dimensional structure of the extracellular binding domains of the apical sodium-dependent bile acid transporter (SLC10A2). Biochemistry 43:11380–11392